Design of Genetic Algorithm Based Fuzzy Controller for Buck-Boost DC-DC Converters

Debela Nugusa Regasa

A Thesis Submitted to

The Department of Electrical Power and Control Engineering

School of Electrical Engineering and Computing

Presented in Partial Fulfillment of the Requirement for the Master of Science

Degree in Electrical Power and Control Engineering (Control Engineering)

Office of Graduate Studies

Adama Science and Technology University

AUG, 2021

Adama, Ethiopia

Design of Genetic Algorithm Based Fuzzy Controller for Buck-Boost DC-DC Converters

Debela Nugusa Regasa

Advisor:

Dr. Tefera Terefe Yetayew

A Thesis Submitted to

The Department of Electrical Power and Control Engineering

School of Electrical Engineering and Computing

Presented in Partial Fulfillment of the Requirement for the Master of Science

Degree in Electrical Power and Control Engineering (Control Engineering)

Office of Graduate Studies

Adama Science and Technology University

AUG, 2021

Adama, Ethiopia

Declaration

I hereby declare that this Master Thesis entitled "Design of Genetic Algorithm Based Fuzzy Controller for Buck-Boost DC-DC Converters" is my original work. That is, it has not been submitted for the award of any academic degree, diploma or certificate in any other university. All sources of materials that are used for this thesis have been duly acknowledged through citation.

______________________ ____________________ ______________

Name of the student Signature Date

Recommendation

I, the advisor of this thesis, hereby certify that I have read the revised version of the thesis entitled "Design of Genetic Algorithm Based Fuzzy Controller for Buck-Boost DC-DC Converters" prepared under my guidance by Debela Nugusa Regasa submitted in partial fulfillment of the requirements for the degree of Mater's of Science in Control Engineering.

Therefore, I recommend the submission of revised version of the thesis to the department following the applicable procedures.

_________________________	__________________	______________
Major Advisor	Signature	Date

Approval sheet

I, the advisors of the thesis entitled "Design of Genetic Algorithm Based Fuzzy Controller for Buck-Boost DC-DC Converters" and developed by Debela Nugusa Regasa, hereby certify that the recommendation and suggestions made by the board of examiners are appropriately incorporated into the final version of the thesis.

Major Advisor	Signature	Date

We, the undersigned, members of the Board of Examiners of the thesis by Debela Nugusa Regasa have read and evaluated the thesis entitled "Design of Genetic Algorithm Based Fuzzy Controller for Buck-Boost DC-DC Converters" and examined the candidate during open defense. This is, therefore, to certify that the thesis is accepted for partial fulfillment of the requirement of the degree of Master of Science in control engineering.

Chairperson	Signature	Date
Internal Examiner	Signature	Date
External Examiner	Signature	Date

Finally, approval and acceptance of the thesis is contingent upon submission of its final copy to the Office of Postgraduate Studies (OPGS) through the Department Graduate Council (DGC) and School Graduate Committee (SGC).

Department Head	Signature	Date
School Dean	Signature	Date
Office of Postgraduate Studies, Dean	Signature	Date

Acknowledgement

First and foremost, I want to express my gratitude to the Almighty God for allowing me to complete my thesis. I would like to express my sincere gratitude to my advisor, Dr. Tefera Terefe Yetayew, who has encouraged me throughout my thesis work and sacrificed his valuable time to encourage me, to work in my way, and to give me the freedom to explore deeply in this study; without his invaluable assistance, it would not have been possible to achieve the study's ultimate goal.

In addition, I like to express my gratitude to the EPCE department head, Mr. Mesfin Merga (MSc.), and laboratory staff members for encouraging me, making open computer labs for discussion when I have a meeting with my advisor, providing a very friendly working environment, and making me feel very welcome during my thesis work.

Finally, I am also thankful to my family, friends, and classmates, who have always encouraged and supported me in finishing this thesis. I am grateful to everyone who supported me during my job, offering me encouragement as well as significant assistance.

Contents

List of Table

List of Figure

List of Acronyms and Abbreviations

BBC	Buck-Boost Converter
C	Capacitor
CCM	Continuous Conduction Mode
C_{min}	Minimum capacitor
D	Average duty cycle
D	Actual duty cycle
$\tilde{d}$	Small signal variation of the duty cycle
DC	Direct Current
DCM	Discontinuous Conduction Mode
F	Switching frequency
GA	Genetic algorithm
i_C	Actual capacitor current
I_C	Average capacitor current
$\tilde{i}_C$	Small signal variation of the capacitor current
i_L	Actual inductor current
I_L	Average inductor current
$\tilde{i}_L$	Small signal variation of the capacitor current
I_{Lmax}	Maximum inductor current
I_{Lmin}	Minimum inductor current
K_d	Derivative gain
K_i	Integral gain
K_p	Proportional gain
L	Inductor
L_{min}	Minimum inductor
R	Load resistor

S	Switch
SMC	Sliding Mode Control
T	Switching period
V_C	Average capacitor voltage
v_C	Actual capacitor voltage
$\tilde{v}_C$	Small signal variation of the capacitor voltage
V_{IN}	Average input voltage
v_{in}	Actual input voltage
$\tilde{v}_{in}$	Small signal variation of the input voltage
V_L	Average inductor voltage
v_L	Actual inductor
$\tilde{v}_L$	Small signal variation of the inductor
V_O	Average output voltage
v_O	Actual output voltage
$\tilde{v}_O$	Small signal variation of output voltage
V_{ref}	Reference voltage
ω_n	Natural frequency
ξ	Damping ratio

Abstract

Switch-mode DC-DC converters convert a direct DC input voltage to a regulated DC output voltage quickly and effectively. Solid-state devices such as transistors and diodes are used in switching power sources to act as a switch, turning on or off completely. Capacitors and inductors, among other energy storage elements, are used for energy transfer and serves as a low-pass filter. So far, this has forced the use of more advanced control mechanisms to fulfill the actual demand. For the control of DC-DC converters, a variety of control approaches have been developed. This converter output voltage usually has oscillation, large overshoot, and takes a long time to settle. It is also unable to provide the desired output voltage when the input voltage and load change. Because of their simplicity, PID controllers are commonly used to acquire the desired output voltage from converters. However, in the case of non-linear systems, the use of a PID controller is not reliable or satisfactory. To improve system performance, non-linear controls are required. The proposed GA, GA-Fuzzy controller, sliding mode controller based on the specified convergence method are proposed and designed in this thesis to achieve fast and stable buck-boost converter performance. The transfer function and mathematical representation of a DC-DC buck-boost converter for duty ratio and input change will be obtained. In MATLAB/Simulink, the modeled system, GA, GA-Fuzzy, and sliding mode controller are implemented. It is clear that GA-fuzzy, control gives the desired output voltage more rapidly than GA-PID and SM control. GA-fuzzy control has a relatively small rising and settling time, but SM control has a long rise and settling time. The overshoot is reduced from 29.6 % to 0.132% when using GA-fuzzy controller, from 29.6% to 0.515% when using GA-PID controller, and from 29.6% to 0.312% when using sliding mode controller. GA-fuzzy controller is insensitive to the input voltage and resistance variation In terms of performance, the proposed control mechanisms are compared. The effectiveness of controllers is also tested under the influence of a random external disturbance

Keywords: *DC-DC Converter, Buck-Boost Converter, SMC, GA, GA-Fuzzy control*

CHAPTER ONE

Introduction

1.1 Background

Day-to-day advancements of technology increases with the desire for power. The everyday activities of civilians necessitate a tremendous amount of power. If the world's population grows, the electricity demand grows as well. To address this issue, conventional power generation techniques must be modernized. With the boo of renewable energy resources, the energy crisis issue is being overcome using modern power electronic components. SMPS, batteries, converters, inverters, and other power electronic circuits are used in power transmission lines to improve the usefulness and productivity of energy sources such as wind, solar, biofuel, biomass, geothermal, and others by storing excess power rather than wasting it. These sources appear to be beneficial in terms of load shifting, customer demand, maximum power generation, and emergency backup[1].

The control of electric power or power condition is not usually used in the form in which it was generated or distributed. many types of power electronics circuits transmit electric energy from a source to a load. One of the most important types is the DC-DC converter. Buck-boost converters, which belong to the DC-DC step-down or step-up converter class, are the most widely used power electronic components in these applications. The importance of high-speed switching, reliability of power conversion with controlled output voltage, and optimum power monitoring abilities enriches its use in a variety of other applications such as electric vehicles, switched power supplies wind energy conversion systems, and any portable device.

The buck-boost converter is made up of only the most common active and passive elements with load[1]; as a result, it is known for its ease of use. Aside from all of these benefits, non-linearity variables in the buck-boost converter, such as delay and hysteresis, cause load variations, power on transients, switching, and electromagnetic interference. Different forms of linear and non-linear controllers are used to solve these issues and maximize the performance for proper power management.

DC-DC converters are electronic circuits that convert a direct source (DC) with a specified voltage level to a different voltage level. They are the most widely used circuits in power electronics. Since all semiconductor parts are powered by DC sources, they can now be found in virtually any electronic device. They are primarily used in all circumstances that need stabilizing input DC voltage to set point[2].

The Buck-Boost converter is one of the most important DC-DC converters. It is a switched-mode power supply with an output voltage that is either lower or higher than the input voltage. The output voltage polarity is the opposite of the input voltage, so it is called an inverting converter. These converters are particularly useful for PV maximum power monitoring and as a step down/up DC transformer, and they are usually used in industrial applications. DC-DC converters usually operate in two modes: continuous and discontinuous. The converter's output current never falls to zero in continuous mode. When the switch is switched off in the discontinuous mode, the output current drops to zero [3].

Switch-mode power supplies make heavy use of DC-DC converters. Switch-mode DC-DC converters are gaining popularity in a variety of fields. This is due to their wide range of applications, which include power supplies for computers, office equipment, appliance control, telecommunications equipment, DC motor drives, automotive, and aircraft, among others [4]. Different types of DC-DC converters are available. Buck converters, boost converters, and buck-boost converters are the most well-known. The buck converter is used for voltage stepdown/reduction, the boost converter is used for voltage step-up, and the buck-boost converter can be used for either step-down or step-up. The buck-boost converter is the subject of this thesis study because it is a common non-isolating power stage topology in which the output voltage is inverted from the input voltage and can be either higher or lower than the input voltage.

DC-DC converters are critical in all voltage levels, including low, medium, and high-power applications. They are much more effective than the old commutator-based method of conversion, and they are built to produce an output within any desired range. Furthermore, DC-DC converters are widely used in the control of electrical drives, one of which is regenerative braking of DC motors, where energy is returned into the supply [5].

Due to the operation of switching components, the output voltage of a buck-boost converter is normally unstable. Because of their simplicity, linear controllers have been used to achieve constant, stable output voltage in this converter, but they are unable to produce the best results when applied to nonlinear systems. As a result, nonlinear control methods that provide the best results in any situation are still in demand. In this thesis, a Genetic-algorithm based fuzzy controller will be designed for a buck-boost converter to achieve a steady, stable output voltage and a fast response time.

1.2 Statement of the Problem

A controller is used in a DC-DC converter to control the converter's operation and achieve regulated output, increased efficiency, and a smooth transition despite changes in input voltage or load conditions. The control laws for DC-DC converters were derived using mathematical linear control theory. The DC-DC converter's switching technique, on the other hand, makes the system nonlinear. To improve the DC-DC converter's performance, intelligent controllers have been used. These controllers use various strategies; some require offline training, while others are complex and time-consuming, with significant overshoot and a long settling time, which characterize the performance of other controllers. As a result, in this thesis, a Genetic algorithm-based fuzzy logic controller for buck-boost converters will be designed to improve converter efficiency. Finally, this study aims to determine which of the controller models is best suited for the converter.

1.3 Objectives

1.3. 1 General Objective:

- The general objective of this thesis is to design a Genetic-algorithm based fuzzy controller for voltage control of DC-DC buck-boost converter.

1.3.2 Specific Objective:

- To the model of DC-DC buck-boost converter
- To design a Genetic-algorithm based fuzzy controller for voltage regulation of buck-boost converter.
- To evaluate the effectiveness of the proposed Genetic-algorithm based fuzzy controller by implementing it on MATLAB/Simulink.
- Compare GA-fuzzy with GA-PID and Sliding mode controller depend on their output simulation results and suggest a better control strategy for the buck-boost converter.

1.4 The scope

The scope of this research is modeling, design, and simulate DC-DC buck-boost converters using GA-fuzzy, GA-PID, and sliding mode controller. All of the models are implemented in the simulation method only using MATLAB/ Simulink software. The effectiveness of these controllers are studied in terms of maximum overshoot, rise time (tr), settling time (ts) and voltage deviations from desired value under input voltage and Load variations.

1.5 Limitation of the thesis

The thesis is restricted to simulating the system using MATLAB/Simulink and demonstrating how the various system components communicate with one another. This is due to the difficulty in obtaining the necessary components for the implementation of a real system. It also includes the extra time and money spent on prototyping and implementing the prototype.

1.6. Motivation of the Study

Switched mode dc-dc converters are among the most basic power electronic circuits, converting one degree of electrical voltage to another by switching action. These converters have received a lot of need in a many places. This is due to their diverse range of applications, which include power supplies for personal computers, office equipment, appliance control, telecommunications equipment, DC motor drives, automotive, and aircraft, among others. Switching converter research, regulation, and stabilization are the most important factors to remember. Switch mode dc-dc converters are controlled using a variety of methods, but the simple and low-cost controller structure is still in demand for most industrial and high-performance applications. Every control method has certain benefits and disadvantages that make it a better control method under some conditions than other control methods.

The control method that provides the best results in any circumstance is always in demand. Pulse width modulated (PWM) voltage mode control, PWM current mode control with proportional (P), proportional integral (PI), and proportional integral derivative (PID) controllers are the most popular control methods for dc-dc converters. P, PI, and PID are examples of traditional control methods that are unable to function satisfactorily under significant parameter or load variations. As a result, nonlinear controllers are used to power dc-dc converters. The ability of these nonlinear controllers to respond quickly to a transient state is one of their main advantages.

1.7 Significance of the Thesis

Any control research is measured by the value added and how it improves the existing process. The expected outcome of this research is improving the performance indices of DC-DC buck-boost converter such as, Overshoot, settling time, rise time etc. The significance of this research is increasing the quality of devices or systems, which use a buck-boost converter in their system.

1.8. Thesis Organization

This thesis organized as follows:

The first chapter summarizes the study's overall context. This chapter covers the most important aspects of the analysis, such as the problem statement, thesis objective, thesis significance, thesis scope, methods used to complete this thesis, and thesis organization.

Chapter 2: discussed the literature review (related works) of existing research work.

Chapter 3: Provides general information on the buck boost converter as well as methodology (mathematical modeling of buck-boost converter)

The results of the buck boost converter with and without the GA-fuzzy controller will be present in Chapter 4. The performance of the GA-PID, GA-fuzzy controller and the sliding mode controller is also contrasted.

Conclusion and recommendations for future research are presented in Chapter 5. At the end of this study paper, you will find a list of referenced references as well as supporting appendices

CHAPTER TWO

Literature Review and Basic Theory

2.1 Related Work

DC-DC switch mode converter mode electronic circuit is vital role to convert a voltage from higher to lower level. DC-DC switching type converters are commonly used and one of the best power electronics circuits, which convert unregulated electrical voltage from one level to regulate desired. Therefore, more analysis, control and stabilization of switching DC-DC converters are the main factors that need to be considered to perform best control system. Many control methods are used for control of switch mode DC-DC converters and the simple and low-cost controller structure are always in demand for most industrial and high-performance applications. Every control method has some advantages and drawbacks due to which that particular control method considers as a suitable control method under specific conditions, compared to other control methods. The control method that gives the best performances under any conditions is always in demand.

Muhanad D. Almawlawe, Marko Kovandzic (2016) presents A Modified Method for Tuning PID Controller for Buck-Boost Converter. This study proposes a design and simulation of a simpler way for developing a proportional–integral–derivative (PID)controller for the Buck-Boost converter that operates in continuous conduction mode. This approach provides good voltage control and is suited for Buck-Boost Dc-Dc converters; nevertheless, it is subject to large variances that may lead this system to deviate from nominal conditions due to line changes and input parameter changes. According to simulation results, this PID controller provides good voltage regulation and is suited for Buck-Boost applications. The obtained results demonstrate the proposed Controller's robustness, and the controlled output of the converter was investigated[6].

In [7] Marouani et al.,2012 found that Sliding Mode Controller for Buck-Boost dc-dc Converter in PV Grid-Connected System. This converter is controlled by the sliding mode control SMC to track the dc reference voltage required by the main grid. The second stage is composed by a dc-bus and a three phase voltage inverter used to interface the GPV with the grid utility. The sliding mode control permits to the dc-dc controller the tracking of the reference direct voltage required by the grid. The direct power control applied to the inverter permits to inject to the grid a three phase equilibrated currents system with low harmonic distortion.

S. Mahalakshmi, Kumar Vasanth P., Muniraj N. J. R (2017) proposed Sliding Mode Controller with Modified Sliding Function of Buck Converter Dc-Dc. The controller offers advantage such as fixed switching frequency and zero steady state error and give a better small signal performance at the designed operating point but under large parameter and load variation their performance degrades so sliding mode control technique are well suited to dc-dc converter as they are inherently variable structure system. The SMC with the proposed sliding surface for a DC-DC buck convertor eliminates the steady state error in the load voltage [8].

Ammar Falah Algamluoli, Haider Abbas Hasan (2020) have been presented Voltage Controller of DC-DC Buck Boost Converter with Proposed PID Controller. This proposed, dc –dc power converter are required controller for current and output voltage to make controller more robustness. In addition, PID controller are designed for load current of buck boost converter and PID for output voltage buck boost converter are investigate. As result, buck boost converter has been designed and implemented to improve that system arrived steady state very fast after making PID controller for current and for load voltage. where, the system with load current PID controller reached steady state at 0.3 S, while, the system with load voltage PID controller reached steady state at 0.15 S [9].

Hanifi Guldemir (2011) has presented Sliding Mode Control of Dc-Dc Buck Converter. In this paper, a robust sliding mode controller for the control of dc-dc buck converter is designed and analyzed. Therefore, the system achieves a robust output voltage against load disturbances and input voltage variations to guarantee the output voltage to feed the load without instability. Robustness and good dynamic behavior is achieved even for large supply and load variations [10].

Sandeep Tyagi, Garima Verma (2018) proposed DC-DC Boost Converter Using Sliding Mode Controller under Variable Conditions. The proposed work is to resolve this problem by using sliding mode controller with modified values of parameters and beta factor for precise values using feedback, close loop system. The input source is taken as DC source voltage at variable conditions. The settling time for SM controller remains nearly same, which is about 3.4 milliseconds for different load therefore the dynamic behavior of the system is basically unaffected by the change in operating conditions [11].

Karthikayini et al.,2015 proposed PWM Sliding Mode Voltage Controller for DC/DC Boost Converters Operating in Continuous Conduction Mode. In this paper, a fixed-frequency PWM-based SM voltage controller has been presented. As a result, converter system acquires the excellent robustness feature of the sliding mode voltage controller; likewise, the fast response capability of a current mode controller. However, the disadvantage of requiring a current sensor is still going on when the controller is constructed using simple analogue IC’s and operational amplifiers [12].

Al-Qaisi et al.,2019 found High performance DC/DC buck converter using sliding mode controller. This paper investigated the performance of the sliding mode control technique for DC/DC converter using frequency response method. In order to optimize the efficiency and for convenient power management, the issues like power on transients, the effect of load variation, Switching and Electromagnetic interference (EMI) losses has to be overcome for which controllers are used. In the proposed method, pulse width modulation (PWM) based on proportional-integral-derivative sliding mode voltage controller (PID SMVC) is designed for a buck converter and the response for appropriate control parameters has been obtained. The system stability has been examined and analyzed from the performance characteristics, which shows clearly that the buck converter controlled by the sliding mode controller has fast dynamic response and it is very efficient for various applications [13].

B. Amarendra Reddy, M.S.V. Santosh Kumar (2017) proposed Automated Tuning and Controller Design for DC-DC Boost Converter. In this thesis, Controller is designed using SISO tool. The parameters of controller resulted from this tool is modified using Automated tuning. This automated tuning allows parameter's optimization, parameter's tuning for robust time response and shaping the frequency response for desired bandwidth etc. Here the controller parameters are optimized. The performance of a DC-DC converter is evaluated using original compensator and different possible compensators against input disturbances and load disturbances [14].

Sarvi et al.,2012 have presented general A Sliding Mode Controller for DC/DC Converters. As DC/DC, converters are nonlinear and time-variant systems, the application of linear control techniques for the control of these converters are not suitable. In this paper, a new sliding mode controller is proposed as the indirect control method and compared to a simple direct control method in order to control a buck converter. The proposed indirect sliding mode controller has more good performance as compared with direct sliding mode as well as PID control. The performance of the proposed sliding mode controller is related on suitable selection of its parameter (k). The proposed controller is robust to load and line as well as reference variations. The propose controller can be used to every DC/DC converters [15].

It should be noted most of the designs and implementations in the literature use a Fuzzy logic, PID, and sliding mode controller to regulate the DC-DC converter. This literature has some drawbacks which not considered in their modeling. Those are:

- Effective of disturbance (input voltage and resistance variation)
- Gain parameters using fuzzy logic controller tuned using try and error which consume more time and it's difficult to get optimized gain value
- Sliding Mode Controller designed in works of literature above does not consider chatter effect
- Finally, the controller designed by PID, fuzzy logic has a long rising and settling time which reduces the efficiency of the system

Genetic algorithm-based fuzzy logic and other controller were implemented in this thesis to overcome this gap.

2.2. Overview of DC-DC Converter

DC-DC converters are electronic devices that convert DC electrical power from one voltage level to another. They are an electronic circuit that converts a DC signal from one voltage level to another by storing the input energy and transferring it to the output at a different voltage level. To pass energy from input to output, they use an inductor and a capacitor as energy storage components [16]. DC-DC converters are widely used in switched-mode power supplies (SMPS) and have a wide variety of applications today. They are becoming increasingly relevant in daily life. There are different types of DC-DC converters. The following are the most well known:-

- Buck Converter
- Boost Converter
- Buck-Boost Converter
- Cuk Converter

2.3. Buck -Boost Converter

Buck-Boost converters are a type of switched mode power supply that incorporates the buck converter and boost converter concepts into a single circuit. In power supplies, a buck converter provides a DC output that ranges from 0 V to just below the voltage input. The voltage output of the boost converter can differ from the same voltage as the input to a much higher rate than the input. However, in many applications, such as battery-powered machines, the input voltage can vary significantly, starting at full charge and progressively decreasing as the battery charge is depleted. A Buck regulator would be ideal for keeping the supply voltage constant at full charge, when the battery voltage is higher than the circuit being powered requires. However, as the charge decreases, the input voltage falls below the amount required by the circuit, requiring the battery to be discharged or recharged; at this stage, the boost regulator [17] will be the ideal solution.

By combining the designs of these two regulators, a regulator circuit that can accommodate a wide range of input voltages, both higher and lower than the circuit's requirements, can be installed. Fortunately, both buck and boost converters use very similar parts; they simply need to be rearranged depending on the rate of input voltage. Such benefits are only found in simple buck-boost converters. As a result, a buck-boost converter was chosen. Nonlinearities are introduced in the converters by adjusting equipment and passive components such as inductors and capacitors, and this converter is commonly used for energy management applications. As a result, it is not possible to use linear control methods for evaluation directly. The output voltage of the converter may be higher or lower than the input voltage. It is also known as an inverting converter since the output voltages polarity is always opposite that of the input voltage [17].

The buck-boost topology, also known as a step-up/down power stage, is a typical non-isolated, inverting power stage topology. Power supply designers choose the buck-boost energy step because the output voltage is inverted from the input voltage, and the output voltage may be either greater or lower than the input voltage. The topology gets its name from the fact that it generates an output voltage that is either two orders of magnitude greater (such as a boost energy stage) or two orders of magnitude lower (such as a buck energy stage) than the input voltage [18]. Because of its inherent nonlinearity, the buck-boost converter is a fascinating subject from a control standpoint. Enhancing energy efficiency conversion is one of the design goals for electronic engineers. Switching loss is a critical performance metric for PWM (pulse-width modulation) converters. The buck-boost converter has two switching cycle states in continuous conduction mode. When a transistor (mosfet or IGBT) is turned on and the diode is in the OPEN circuit mode, it is said to be in the ON state. When a transistor (mosfet or IGBT) is turned off and the diode is in the CLOSE circuit mode, it is said to be in the OFF state. Each of the two states can be represented by a simple linear circuit, with the circuit switches being replaced by their corresponding circuit in each state.

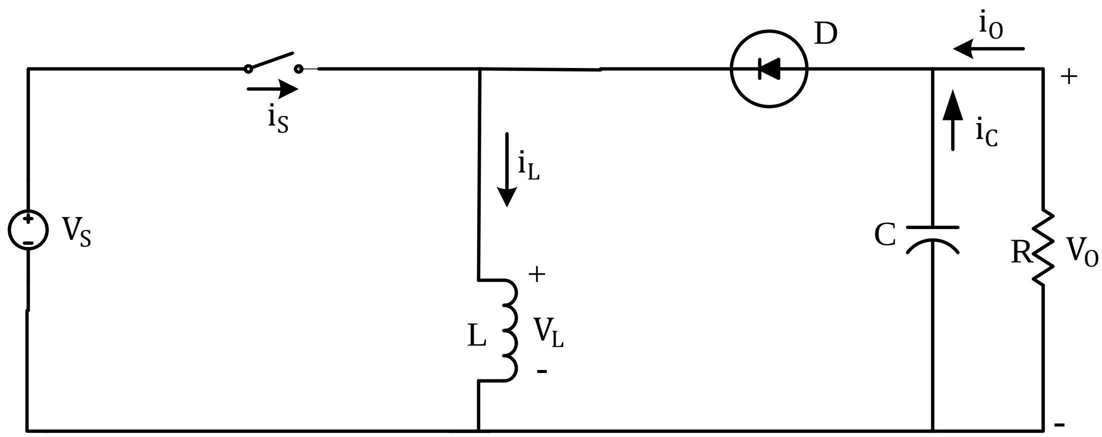

Figure 2.1 buck-boost converter circuit [16].

The duration of the ON state is D × TS = TON where D is the duty cycle, set by the control circuit, expressed as a ratio of the switch ON time to the time of one full switching cycle, Ts(0.01mHz.). The OFF-state period is called TOFF. Since there are only two states per switching cycle for continuous conduction mode, TOFF is equal to (1-D) × TS. The amount (quantity) (1-D) is sometimes referred to as D' [2] The waveforms of buck-boost converter for continuous conduction mode of operation are shown in the Figure 2.2 below.

Alternative and renewable energy conversion, handheld devices, and many industrial processes all depend on DC-DC converters. It is primarily used to convert an unregulated DC source, such as the output of a rectifier, a battery, or a solar cell, into a controlled DC voltage and so on. Nonetheless, the source varies significantly, owing to variations in line voltage, running out of a battery, and so on, but only within a given range. Taking all of this into account, the aim is to maintain a constant voltage when delivering to a large range of loads.

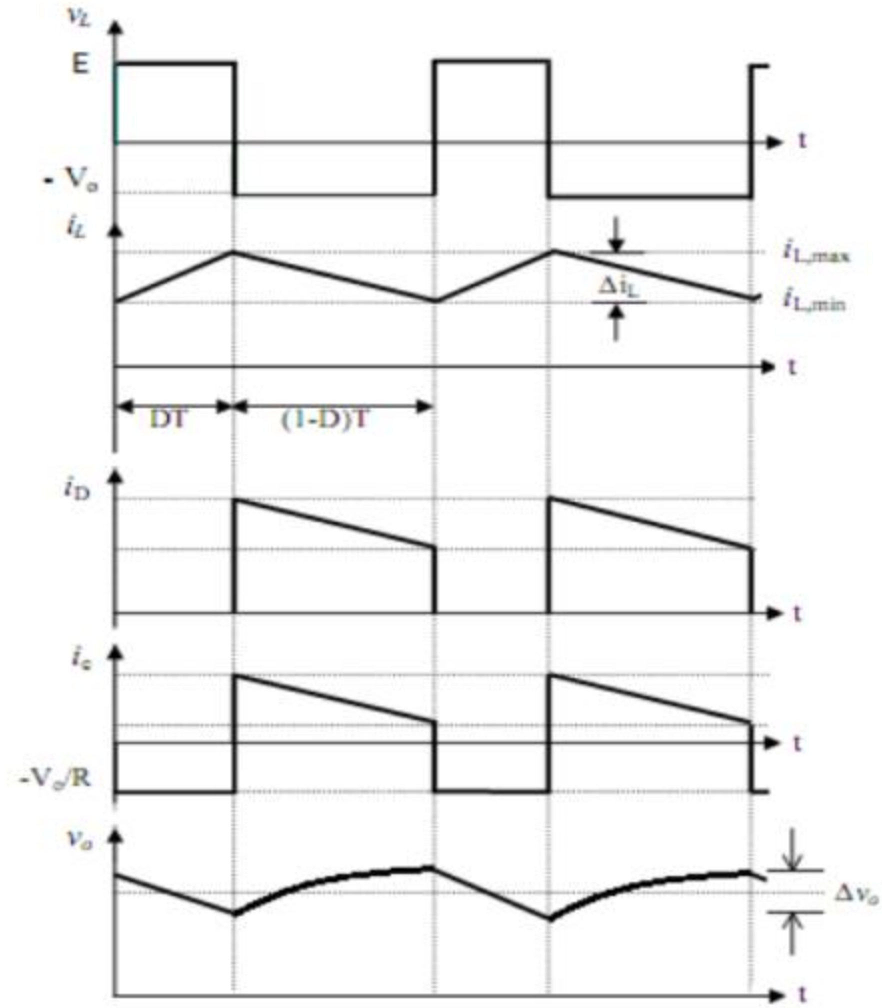

Figure 2.2 Waveforms of buck-boost converter for continuous conduction mode operation [16]

2.4. Buck-Boost Converter Mode of Operation

Based on the continuity of inductor current flow, DC-DC buck-boost converters typically have two modes of operation. There are the following:

- Discontinuous conduction mode (DCM) and
- Continuous conduction mode (CCM)

Mode of continuous conductivity Discontinuous conductive mode and CCM For each switching cycle, DCM refers to whether or not the current in the power storage portion (inductor) reaches zero. Since it never reaches zero in CCM, there is some energy left over at the end of each switching cycle, which is "topped up" in the next cycle to provide enough energy for the output.

In DCM, all of the energy is used up for each loop, and the inductor is left with no current and no stored energy for a portion of the time. The amount of energy stored is proportional to the output load, so whether you are in CCM or the load [3] determines DCM. We can generalize the following in general:

2.4.1. Continuous Conduction Mode

When the current through the inductor never reaches zero, the inductor partially discharges before the switching cycle begins. During a switching time, this condition occurs when the inductor current flow is continuous of charge and discharge. Each switching cycle in CCM is divided into two parts: DT and D'T (D+ D'=1). The inductor current increases and decreases in the first and second modes, DT andD'T, respectively.

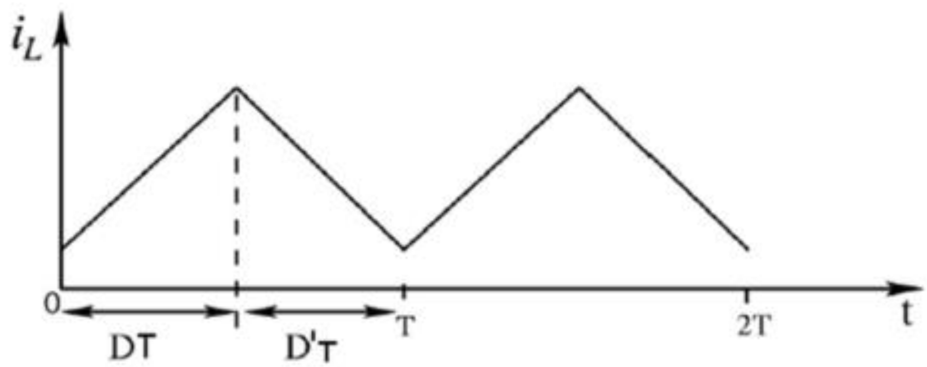

Figure 2.3 Waveform of inductor current for continuous conduction mode [4]

The buck-boost converter operates in continuous conduction mode and has two states per switching cycle: ON and OFF. When the switch is closed and the diode is in reverse biased mode, it is said to be in the ON state. When the switch is open and the diode is forward biased (conducting), it is in the OFF state. Only the continuous conduction mode of the buck-boost converter is considered in this thesis.

2.4.2. Discontinuous Conduction Mode

At the end of the switching cycle, the current through the inductor is zero, indicating that the inductor is fully discharged. During a switching cycle, the inductor current stays at zero for an extended period of time with no charge and discharge. Each switching cycle in the discontinuous conduction mode is divided into three parts: DT, D'T, and D''T (D+D'+D''=1).

The inductor current increases and decreases in the first and second modes, DT and DT, respectively, while the inductor current stays at zero in the third mode, DT, with no charge or discharge.

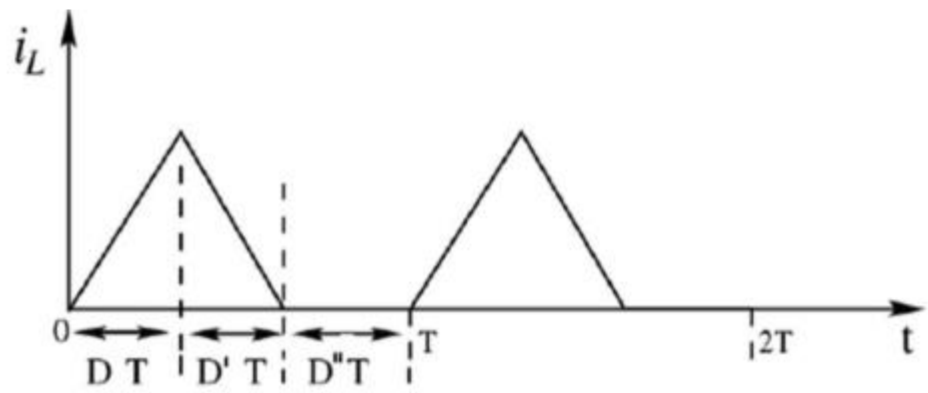

Figure 2.4 Waveform of inductor current for discontinuous conduction mode [4]

2.5. Purpose of Different Components in the Buck-Boost Converter

In a buck-boost converter, various types of components are used. Those are:

- Capacitor
- Inductor
- diode
- switch

A. Capacitor

A system stores energy. The filtering action of the capacitor is provided by providing a path away from the load for harmonic currents. Output capacitance (over the load) is necessary to reduce voltage overshoot and ripple at the output of a step-down / step-up converter. The capacitor is large enough that its voltage does not change significantly when the switch is turned off.

B. Inductor

When the circuit is turned on, the inductor's job is to limit the current slew rate (current in rush) through the power switch. The current flowing through the inductor cannot abruptly shift. When the current through an inductor begins to fall, the inductor acts as a source to keep the current flowing. The main benefit is that the inductor stores energy as it is used to lower voltage. The inductor also decides if the converter is running in continuous conduction mode and monitors the percent of ripple. The smaller inductor value allows for a faster transient response; however, it also creates greater current ripples, which leads to higher conduction losses in the switches, inductor, and parasitic resistances. In addition, a smaller inductor necessitates a larger filter capacitor to reduce output voltage ripple. Switched supply inductors are often wound on toroidal cores, which are sometimes made of ferrite or powdered iron and have a distributed air gap to store electricity.

C. Switch

Since the current in the inductor cannot shift abruptly, the inductor current must have a direction when the switch is turned off (open). The freewheeling diode (catch diode) provides this direction. The aim of this diode is not to rectify, but to direct current flow in the circuit and ensure that current flows into the inductor at all times. It is also essential for this diode to be able to switch off quickly. As a result, the diode allows the converter to transfer the inductor's stored energy to the load. This is why, as compared to a linear regulator, DC-DC Converters have a higher efficiency. The current increases linearly when the switch is closed. When the switch is opened, the freewheeling diode causes a linear drop in current.

D. Switch

The switch's role is to change the converter's topology. The inductor creates and retains energy when it is turned on. Energy is passed to the load when the switch is turned off. A switch may be a toggle switch that toggles between supply voltage and ground in its most basic form. Transistors used in switching power supplies must have fast switching times and be able to withstand voltage spikes caused by the inductor. SCR, GTO, IGBT, and MOSFET are the most popular switching devices. Efficacy High-frequency power systems, such as high-density power supplies, depend heavily on MOSFETs[19]. MOSFETs are therefore used in designs with much higher frequencies but lower voltages.

Operating Frequency

The switching frequency of an inverter or converter is the rate at which the switching unit is turned on and off. The typical frequency ranges from a few KHz to a few megahertz (20KHz-2MHz). Increased switching frequency reduces the size of related components including inductors, transformers, resistors, and condensers, as well as the amount of space required on the board and in the case.

In terms of [19], this frequency has an effect on component selection:

- Physical sizes which becomes smaller at higher frequencies
- Electrical characteristics
- Frequency response

- Minimum On-time
- Power losses and more

The switch's output is determined by its operating frequency. Increased switching frequencies are becoming more popular in research and new power converter designs. The higher the switching frequency, the smaller the physical size and part, and the lower the cost worth. This is done in order to reduce the total size of the power converter even further.

CHAPTER THREE
METHODOLOGY

3.1. Introduction

This chapter covers data collection and analysis, as well as mathematical modeling the DC-DC buck-boost converter. The linear controller is unable to achieve the best output under desired voltage and load variations because the converter is nonlinear. To overcome the disadvantages of linear controllers, nonlinear controller sliding mode controller been developed for buck-boost converters in this chapter. Finally, the system is simulated by using MATLAB/2019a software both in Simulink and in script.

3.2. Materials

Software such as MATLAB/2019b, Microsoft Office 2016, and MathType 6.0 equation are used in this study. MATLAB is a computer computing software that includes technical toolboxes and Simulink. The thesis documentation is edited in Microsoft Office. MathType 6.0 is a Microsoft Word and PowerPoint presentation tool that allows you to write mathematical formulas and equations.

3.3. Methods

The following method have been used for the accomplishment of this thesis:

- **Literature review:** The buck-boost converter control mechanism will be examined in this section. Various literatures related to this thesis work, as well as their control mechanisms, are studied.
- **Modelling of the system:** The purpose of this section is to identify the DC-DC buck-boost converter model and mathematical model.
- **Design controller**: The next stage will be to design a controller using GA-PID,GA-fuzzy and a sliding mode controller after the system model has been obtained.
- **Simulation and evaluation of controllers:** The next step is to simulate the system using MATLAB after the modeling and design phase is completed.
- **Documentation and conclusion:** After the simulation of the proposed models, the discussion section compares the controllers, summarizes the findings, and concludes up the paper. The following procedures are followed to complete this thesis, and the general technique is described in the chart shown in Fig.3.1.

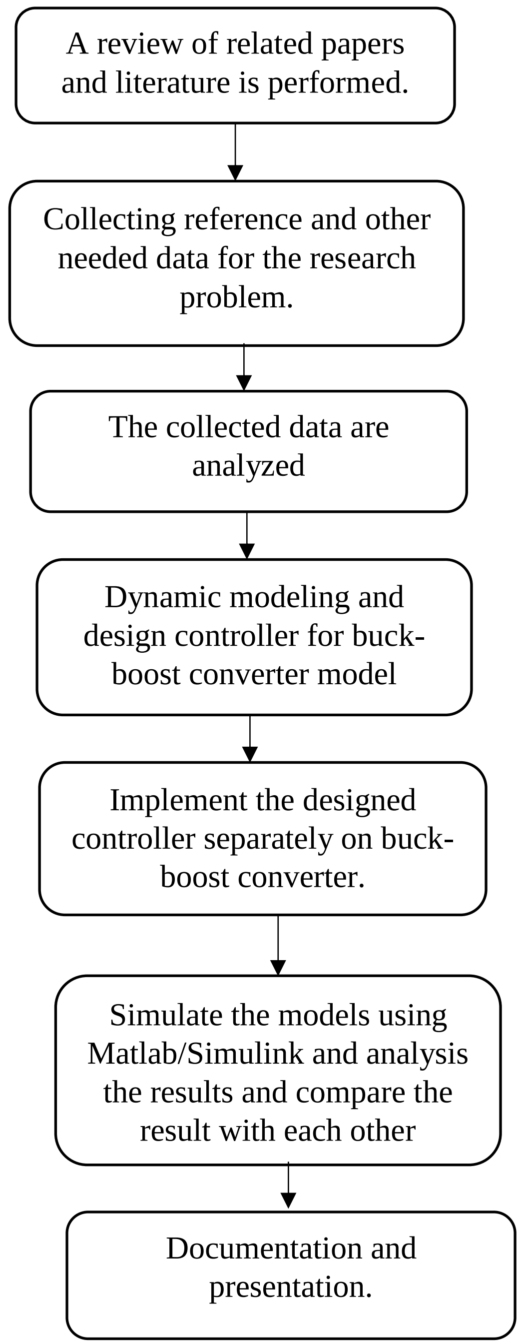

Figure 3.1 Block diagram of the research methodology

3.4 Buck-Boost Converter Analysis

It is possible to measure the following using Kirchhoff's voltage and current laws based on the buck-boost converter analysis for the switch closed and open.

3.4.1. Calculation for Duty Ratio

First, assume that the converter is in steady state when calculating the duty ratio. The switches are considered as being perfect, and the losses in the inductive and the capacitive components are ignored. It is also worth noting that the following review excludes any parasitic resistances (everything is an ideal case). The study also assumes that the converter is only in continuous conduction mode, which means that the inductor current is greater than zero. To calculate the duty ratio, a two-state buck-boost converter must be analyzed.

3.4.2. Buck-Boost Converter Analysis for the Switch Closed (ON)

When the switch is closed, the corresponding circuit of a buck-boost converter is shown below.

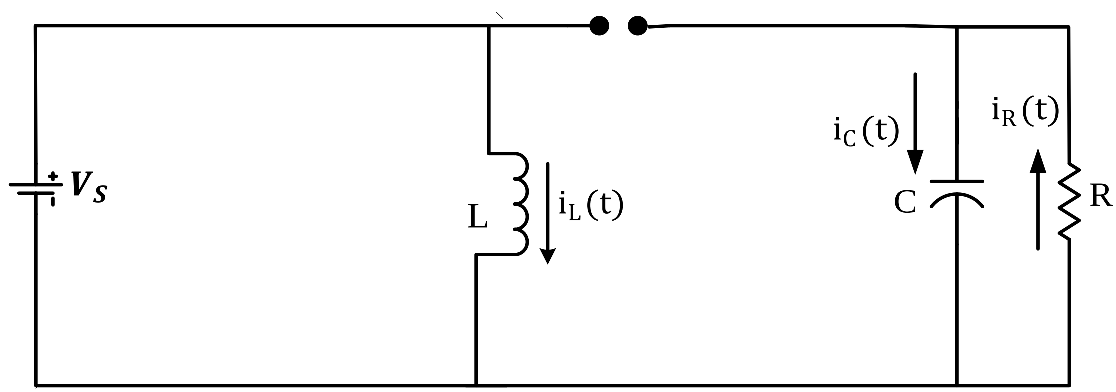

Figure 3.2 Buck-Boost converter circuit when the switch is closed (Boost operation)

When the switch is closed (ON) for lot of time, the inductor current is conducted and the diode becomes reverse biased. Therefore, a positive voltage is produced across the inductor.

$$V_s = V_{in=} L \frac{di_L(t)}{dt} \quad (3.1)$$

Equation (3.2) can be written in the following way:

$$\frac{\Delta i_L}{\Delta t} = \frac{V_{in}}{L} \quad (3.2)$$

Equation (3.2) is given as, since the amount of time when the switch is turned on is given as: $\Delta t = \text{DT}$.

$$\Delta i_L(\text{Closed}) = \left(\frac{V_{in}}{L}\right)\text{DT} \tag{3. 3}$$

where, D= duty ratio.

3.4.3. Buck-Boost Converter Analysis for the Switch Open (OFF)

When the switch is open and the diode is forward biased or in the conducting state, the corresponding circuit of a buck-boost converter is shown below.

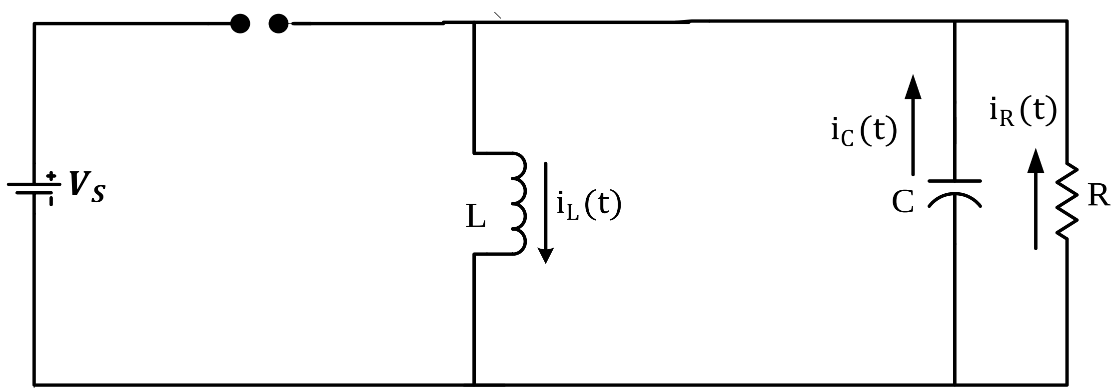

Figure 3.3 Buck-Boost converter circuit when the switch is open

Because of the inductive energy storage, inductor current continues to flow even though the switch is turned off. The diode is forward biase at this time, and current flows through it.

$$L\frac{di_L(t)}{dt} = -V_C - V_o \tag{3. 4}$$

Equation (3.4) can be written in the following way:

$$\frac{\Delta i_L}{\Delta t} = \frac{V_o}{L} \tag{3. 5}$$

Since the duration of time when the switch OFF is given as Δt = (1 - D) T, Equation (3.5) is given as,

$$\Delta i_L(\text{Open}) = -\frac{V_o(1-D)\,T}{L} \tag{3. 6}$$

The net change in inductor current over one period must be zero for steady state operation

$$\Delta i_L(\text{Open}) + \Delta i_L(\text{Closed}) = 0 \tag{3. 7}$$

Equation (3.7) is obtained by substituting Equations (3.3) and (3.6) into Equation (3.7) and simplifying it.

$$\mathrm{D} = -\frac{V_o}{V_{in}}(1 - \mathrm{DT}) \tag{3. 8}$$

We can get, by solving for $\mathrm{V_o}$,

$$\mathrm{V_o} = -\frac{D}{(1-D)}\mathrm{V_{in}} \tag{3. 9}$$

In comparison to the input voltage, Equation 3.9 shows the output voltage provided by the buck-boost converter process. Depending on the duty cycle, this converter will generate three stages of voltage [2].

- If the duty cycle is greater than 0.5 (D > 0.5), the output voltage will be higher than the input voltage (boost mode).
- If the duty cycle is equal to 0.5 (D = 0.5), the output will produce the same amount of voltage as input voltage
- If the duty cycle is lower than 0.5 (D < 0.5), the output voltage will be lower than the input voltage (buck mode).

The source is never directly connected to the load while using a buck-boost converter. While the switch is closed, energy is stored in the inductor, and when it is opened, energy is transferred to the load. Because of this, the buck boost converter is also known as an indirect converter. In other words, since the waveform must repeat from one-time period to the next in steady-state action, the integral of the inductor voltage VL over one-time period must be zero.

$$\int_0^T V_L\, dt = \int_0^{\mathrm{t_{on}}} V_L\, dt + \int_{\mathrm{t_{on}}}^T V_L\, dt = 0 \tag{3. 10}$$

T is the switching time (i.e. T = t_{on} +t_{off}), and integrating over it gives

$$(V_{in} - \mathrm{V}_{\boldsymbol{o}})\, t_{on} = \mathrm{V}_{\boldsymbol{o}}(\,\mathrm{T} - t_{on}) \tag{3. 11}$$

Equation (3.11) can be simplified as follows:

$$D = -\frac{V_o}{V_{in}}(1 - \mathrm{D}) = \frac{t_{on}}{T}\ (1 - \mathrm{D}) \tag{3. 12}$$

3.4.4. Calculation for Inductor

Assuming no power losses in the converter, the load must consume the same amount of power as the source.

$$\mathrm{P_o} = \mathrm{P_s} \tag{3. 13}$$

Equation (3.13) can be written as,

$$\frac{\mathrm{V^2{}_O}}{\mathrm{R}} = \mathrm{V_{in}I_s} \tag{3. 14}$$

The average source current is proportional to the average inductor current as follows:

$$\mathrm{I_s} = \mathrm{I_L D} \tag{3. 15}$$

Thus, Equation 3.14 can be written as,

$$\frac{\mathrm{V^2{}_O}}{\mathrm{R}} = \mathrm{V_{in}I_L D} \tag{3. 16}$$

Solving I_L for Equation (3.16) is as follows:

$$\mathrm{I_L} = \frac{\mathrm{V^2{}_O}}{\mathrm{V_{in}DR}} = \frac{P_{\mathrm{o}}}{\mathrm{V_{in}D}} \tag{3. 17}$$

$$\mathrm{I_L} = \frac{\mathrm{V_S D}}{\mathrm{R(1 - D)^2}} \tag{3. 18}$$

For continuous current mode I_L must be greater than ΔI_L.

The following are the maximum and minimal inductor currents:

$$\mathrm{I_{Lmax}} = \mathrm{I_L} + \frac{\Delta \mathrm{I_L}}{2} \tag{3. 19}$$

$$\mathrm{I_{Lmin}} = \mathrm{I_L} - \frac{\Delta \mathrm{I_L}}{2} \tag{3. 20}$$

Substituting for I_L and ΔI_L from Equation (3.18) and (3.3) into Equations (3.19) and (3.20), respectively, and simplifying gives

$$I_{Lmax} = \frac{V_S D}{R(1-D)^2} + \frac{V_{in} DT}{2L} \tag{3. 21}$$

$$I_{Lmin} = \frac{V_S D}{R(1-D)^2} - \frac{V_{in} DT}{2L} \tag{3. 22}$$

The inductor current must remain positive for continuous current to flow. As a result, the minimum inductor current is set to zero to establish the boundary between continuous and discontinuous conduction modes.

$$I_{Lmin} = \frac{V_S D}{R(1-D)^2} - \frac{V_{in} DT}{2L} \tag{3. 23}$$

Thus, rearranging and solving for the inductor from Equation (3.23) yields the value of the inductor that defines the boundary between the CCM and the DCM.

$$L_{min} = \frac{R(1-D)^2}{2F} R \tag{3. 24}$$

where f is the switching frequency ($f = \frac{1}{T}$)

This is the inductor value that defines the operation boundary between CCM and DCM. As a result, the value of the inductor used in the buck-boost converter must be greater than the minimum value of inductor in order for it to operate in continuous conduction mode.

The ripple inductor current is the difference between the inductor current's maximum and minimum values.

$$\Delta I_L = I_{Lmax} - I_{Lmin} \tag{3. 25}$$

Equation (3.25) is obtained by substituting for I_{Lmax} and I_{Lmin} from Equations (3.21) and (3.22), respectively, and simplifying.

$$\Delta I_L = \frac{V_{in} DT}{L} \tag{3. 26}$$

3.4.5. Calculation for Capacitor

The output capacitor is supposed to be sufficiently high to ensure that the output voltage remains constant. However, considering the waveform shown in Figure above for continuous conduction mode of operation, the ripple in the output voltage (ΔV_O) with a practical value of capacitance can be determined. If the entire ripple component of the inductor current (I_L) flows through the capacitor and the average component through the load resistor, the maximum increase in charge (Q) stored in filter capacitor C equals triangle region. As a result, the triangle area shown in Figure is obtained by measurement for each cycle [20].

$$\Delta V_O = \frac{\Delta Q}{C} \tag{3. 27}$$

$$\Delta Q = \frac{1}{2}\frac{T}{2}\frac{\Delta I_L}{2} \tag{3. 28}$$

Equation (3.27) is obtained by substituting for from Equation (3.28).

$$\Delta V_O = \frac{1}{2}\frac{1}{C}\frac{T}{2}\frac{\Delta I_L}{2} \tag{3. 29}$$

Rearranging and solving for capacitor by substituting for ΔI_L from Equation (3.26) into Equation (3.29) and substituting for $\Delta I_L$from Equation (3.26) into Equation (3.29)

$$C_{min} = \frac{(1 - D)V_O}{8\Delta V_O L f^2} \tag{3. 30}$$

This is the mandatory minimum capacitance. The filter capacitance must be greater than the minimum capacitance to keep the peak-to-peak value of the ripple voltage below a certain value and to reduce voltage overshoot.

The buck boost converter's output voltage ripple is:

$$|\Delta Q| = \frac{V_O}{R} DT = C\Delta V_O \tag{3. 31}$$

Solving for ΔV_O,

$$\Delta V_O = \frac{V_O\ DT}{RC} = \frac{V_O\ D}{RCf} \tag{3. 32}$$

Thus, we can have,

$$r = \frac{\Delta V_O}{V_O} = \frac{D}{RCf} \tag{3. 33}$$

The switch duty-cycle regulates the buck-boost converter's output voltage. As a result, using a buck-boost converter allows you to achieve outputs of any magnitude. Furthermore, if D=0, the output is zero, if D=1, the output is infinity, and if D=0.5, the output is proportional to the input[21].

3.5. Mathematical Model of Buck-Boost Converter

The state space mathematical model of a DC-DC buck-boost converter is obtained by applying simple laws governing the system's operation. Kirchhoff's voltage and current laws can easily be used to calculate the dynamics of this converter in continuous conduction mode. The following statement has been taken into account:

- The switch is closed for time DT and open for time (1-D)T, where D is duty ratio and T is switching period.
- The circuit operates at steady state.
- The inductor current is continuous (i.e. always positive).
- The capacitor is very large i.e. in order to limit the peak-to-peak value of the ripple voltage below a certain value and to minimize voltage overshoot; it must be greater than the minimum capacitance required for Continuous conduction mode.
- The inductor value must be greater than the minimum inductor to ensure continuous conduction mode and to prevent higher conduction loss in switch, inductor and parasitic resistances.

The basic schematic diagram of Buck-Boost converter is shown in Figure 3.1. The input source internal resistance, inductor series resistance, and capacitor series resistance are represented by r_{in},r_L, and rC, respectively. We suppose that the element values are chosen in such a way that the converter operate in Continuous Current Mode (CCM)

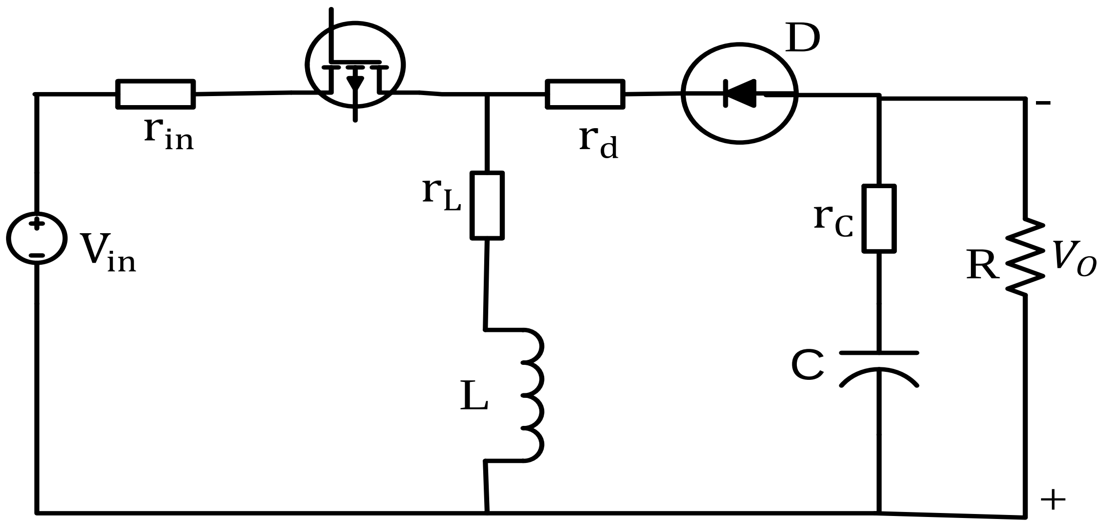

Figure 3.4 Buck-Boost converter diagram

Modeling is done using State-space averaging technique. The state vector for the Buck-Boost converter is defined as $\begin{bmatrix} V_C \\ i_L \end{bmatrix}$ where i_L is the current through an inductor, and V_C is the voltage across the capacitor. The Buck-Boost converter is illustrated by the following set of State space equations in continuous time domain.

$$\left.\begin{aligned} \dot{x}_1(t) &= A_1 x(t) + B_1\ Vs(t), \quad s = 1 \\ \dot{x}_2(t) &= A_2 x(t) + B_2\ Vs(t), \quad s = 0 \end{aligned}\right\} \qquad (3.\ 34)$$

where S = 1 represents ON condition of the switch and S = 0 represents OFF condition of the switch. Implement the double pole double throw switch by one strongly controlled MOSFET switch S and one passive diode D controlled by the current in the circuit, so that the switch S and diode D are always in complementary state as shown in Figure 3.2. The switch S is turned ON/OFF by control signals only.

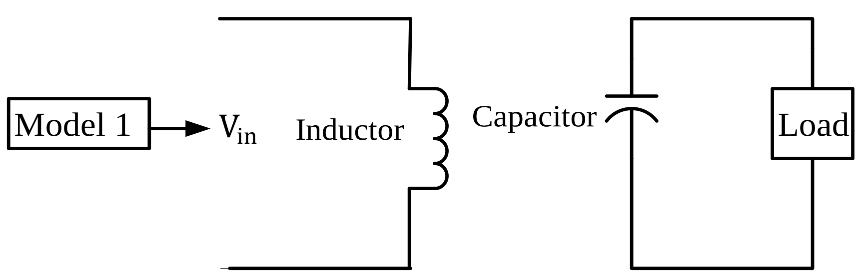

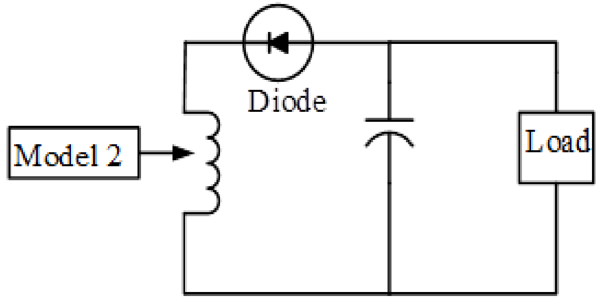

Figure 3.5 Equivalent circuit of Buck-Boost converter

Mode 1: when the switch is closed and the diode is reverse biased

When MOSFET switch S is ON, output voltage V_O is negative hence diode D is OFF (reverse biased) and load is not connected to input. The input current flows through the transistor and inductor. When gate pulses are high, MOSFETs close, as seen in Fig. 3.5. Due to the periodic nature of gate pulses, this occurs when n.T < t < n.T + d.T, n = 0, 1, 2, 3 …. Therefore, MOSFET is closed for d.T seconds [22]. The equivalent circuit of Buck-Boost converter for mode 1 is shown in Fig. 3.6.

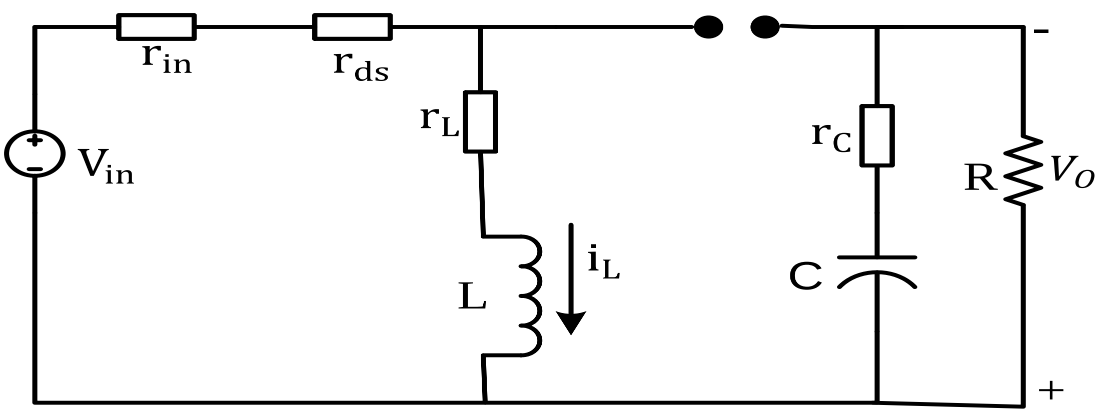

Figure 3.6 Buck-Boost converter when the switch is closed

The differential equations related to state variables are, applying Kirchhoff's voltage and current law to the mode-1 circuit is as follows.

$$\begin{cases} v_{in} = (r_{in} + r_{ds} + r_L)i_L + \dfrac{Ldi_L}{dt} \\ r_C \dfrac{Cdv_C}{dt} + v_C = -R\dfrac{Cdv_C}{dt} \end{cases} \tag{3. 35}$$

Then to obtain state equations rearranging equation (3.35) and simplified using simple algebraic manipulations,

$$\begin{cases} \dfrac{Ldi_L}{dt} = -(r_{in} + r_{ds} + r_L)i_L + v_{in} \\ \dfrac{Cdv_C}{dt} = -\dfrac{v_C}{r_C + R} \end{cases} \tag{3. 36}$$

Output equation v_O can be given as:

$$v_O = -R\frac{Cdv_C}{dt} = \frac{Rv_C}{r_C + R} \tag{3. 37}$$

Equation (3.37) and (3.36) can be written as:

$$\left.\begin{aligned} \frac{dx(t)}{dt} &= A_1x(t) + B_1u(t) \\ y(t) &= C_1x(t) + D_1u(t) \end{aligned}\right\} \tag{3. 38}$$

where, $A_1 = \begin{bmatrix} -\frac{1}{L}(r_{in} + r_{ds} + r_L) & 0 \\ 0 & -\frac{v_C}{C(r_C+R)} \end{bmatrix}$ $B_1 = \begin{bmatrix} 0 \\ \frac{1}{L} \end{bmatrix}$ and $C_1 = \begin{bmatrix} 0 & \frac{R}{r_C+R} \end{bmatrix}$

The variables x(t), u (t) and y(t) are the state variables consisting of output voltages and inductor currents, input voltages to the converter and output voltages respectively

Mode 2: when the switch is open and the diode is forward biased (conducting state)

During mode 2 operation switch S is OFF as set by external control signal applied to switch S

Since $i_L = \int \frac{V_L}{L} dt$, no need to actively control the diode D with any control signals then it is automatically turned ON by i_L, when it flows to the left and turned OFF, when i_L flows to the right. As shown in Fig. 3.6, when gate pulses are low, MOSFETs open (i.e., logic level zero). This occurs when n.T +d.T < t < (n +1). T +d.T, n = 0, 1, 2, 3, …. Because gate pulses are periodic. As a result, the MOSFET is open for (1-d).T seconds [22].

The equivalent circuit of Buck-Boost converter during mode 2 operation is shown in above

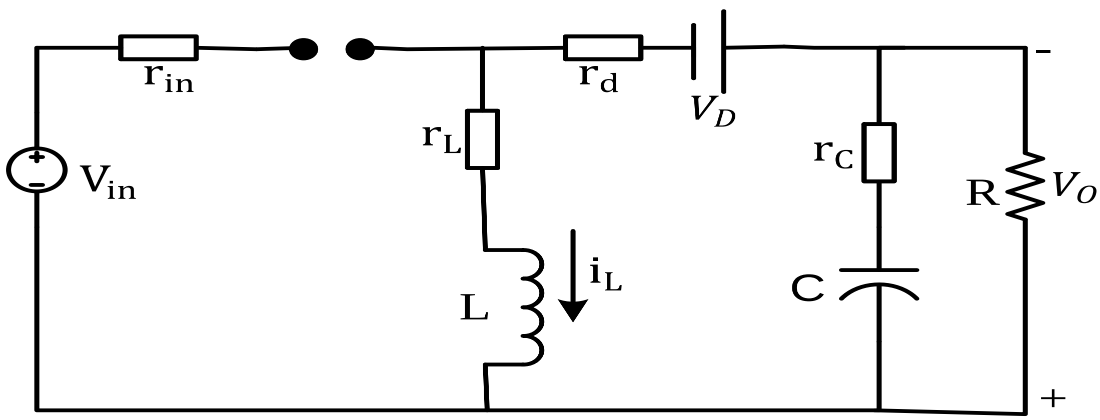

Figure 3.7 Buck-Boost converter when the switch is open

Applying Kirchhoff's voltage and current law to the mode 2 equivalent circuit:

$$\begin{cases} L\dfrac{di_L}{dt} + (r_L + r_d)i_L + V_D + r_C\dfrac{Cdv_C}{dt} + v_C = 0 \\ r_C\dfrac{Cdv_C}{dt} + v_C = R\left(i_L - \dfrac{Cdv_C}{dt}\right) \end{cases} \tag{3. 39}$$

Equations (3.39) can be rearranged and simplified using simple algebraic manipulations:

$$\begin{cases} L\dfrac{di_L}{dt} = -(r_L + r_d)i_L - V_D - \dfrac{r_C R i_L}{r_C + R} - \dfrac{Rv_C}{r_C + R} \\ \dfrac{Cdv_C}{dt} = \dfrac{Ri_L}{r_C + R} - \dfrac{v_C}{r_C + R} \end{cases} \tag{3. 40}$$

Output v_O equation can be given as:

$$v_O = R\left(i_L - \frac{Cdv_C}{dt}\right) = R\left(\frac{r_C i_L}{r_C + R} + \frac{v_C}{r_C + R}\right) \tag{3. 41}$$

$$\left.\begin{aligned} \frac{dx(t)}{dt} &= A_2x(t) + B_2u(t) \\ y(t) &= C_2x(t) + D_2u(t) \end{aligned}\right\} \tag{3. 42}$$

where, $A_2 = \begin{bmatrix} -\frac{1}{L}\left(r_L + r_d + \frac{r_C R}{r_C+R}\right) & \frac{-R}{L(r_C+R)} \\ \frac{R}{C(r_C+R)} & \frac{-1}{C(r_C+R)} \end{bmatrix}$ $B_2 = \begin{bmatrix} 0 \\ 0 \end{bmatrix}$ and $C_2 = \begin{bmatrix} \frac{Rr_C}{r_C+R} & \frac{1}{r_C+R} \end{bmatrix}$ assume that $V_D = 0$

3.6. State Space Average Model of Buck-Boost Converter

A state space average model is obtained by averaging the state equation derived above over switching cycle. Perform state-space averaging using the duty cycle as a weighting factor and combine state equations into a single averaged state equation. Averaging is used to superimpose the results of previous analyses. The MOSFET closes for d.T seconds and then opens for (1-d).T seconds. As a result, it is reasonable to multiply the derived equation set by the valid and averaged period length. Then inductor averaged equation is given as follow:

$$\begin{cases} \frac{Ldi_L}{dt} = -(r_{in} + r_{ds} + r_L)i_L + v_{in}, n.T < t < n.T + d.T \\ L\frac{di_L}{dt} = -(r_L + r_d)i_L - V_D - \frac{r_C R i_L}{r_C + R} - \frac{Rv_C}{r_C + R}, n.T + d.T < t < (n+1)T. \end{cases} \tag{3. 43}$$

The left and right sides of the equations multiply the length of the time interval.

$$\begin{cases} \frac{Ldi_L}{dt} \times d.T = (-(r_{in} + r_{ds} + r_L)i_L + v_{in}) \times d.T \\ L\frac{di_L}{dt} \times (1-d).T = (-(r_L + r_d)i_L - V_D - \frac{r_C R i_L}{r_C + R} - \frac{Rv_C}{r_C + R}) \times (1-d).T \end{cases} \tag{3. 44}$$

The sides that correspond are added together and multiplying both sides by 1/T provides averaging.

$$d \times \frac{Ldi_L}{dt} + (1-d) \times L\frac{di_L}{dt} = d \times (-(r_{in} + r_{ds} + r_L)i_L + v_{in}) + (1-d) \times (-(r_L + r_d)i_L - V_D - \frac{r_C R i_L}{r_C + R} - \frac{Rv_C}{r_C + R}) \tag{3. 45}$$

Applying some basic algebraic operations,

$$\frac{Ldi_L}{dt} = d \times (-(r_{in} + r_{ds} + r_L)i_L) + dv_{in} + (1-d) \times \left(-\left(r_L + r_d + \frac{r_C R i_L}{r_C + R}\right) i_L\right) + (1-d) \times (-\left(V_D + \frac{Rv_C}{r_C + R}\right) \tag{3. 46}$$

Assumed that:

$$R_1 = r_{in} + r_{ds} + r_L \tag{3. 47}$$

$$R_2 = r_L + r_d + \frac{r_C}{r_C + R} \tag{3.48}$$

$$\begin{cases} \frac{Ldi_L}{dt} = -d \times R_1 i_L - (1-d) \times R_2 i_L - (1-d) \times \frac{Rv_C}{r_C + R} - (1-d) \times V_D \\ \quad + dv_{in} \end{cases} \tag{3.49}$$

The capacitor voltage equations can be derived using the same procedure:

$$\begin{cases} \frac{Cdv_C}{dt} = -\frac{v_C}{r_C + R}, n.T < t < n.T + d.T \\ \frac{Cdv_C}{dt} = \frac{Ri_L}{r_C + R} - \frac{v_C}{r_C + R}, n.T + d.T < t < (n+1)T \end{cases} \tag{3.50}$$

The left and right sides of the equations multiply the length of the time interval.

$$\begin{cases} \frac{Cdv_C}{dt} \times d.T = (-\frac{v_C}{r_C + R}) \times d.T \\ \frac{Cdv_C}{dt} \times (1-d).T = (\frac{Ri_L}{r_C + R} - \frac{v_C}{r_C + R}) \times (1-d).T \end{cases} \tag{3.51}$$

The sides that correspond are added together:

$$d.T \times \frac{Cdv_C}{dt} + (1-d).T \times \frac{Cdv_C}{dt} = d.T \times \left(-\frac{v_C}{r_C + R}\right) + (1-d).T \times \left(\frac{Ri_L}{r_C + R} - \frac{v_C}{r_C + R}\right) \tag{3.52}$$

Multiplying both sides by 1/T provides averaging.

$$\frac{Cdv_C}{dt} = d \times \left(-\frac{v_C}{r_C + R}\right) + (1-d) \times \left(\frac{Ri_L}{r_C + R} - \frac{v_C}{r_C + R}\right) \tag{3.53}$$

Applying some basic algebraic operations,

$$\frac{Cdv_C}{dt} = (1-d)\frac{Ri_L}{r_C + R} - \frac{v_C}{r_C + R} \tag{3.54}$$

As a result, the average system equation can be expressed as,

$$\begin{cases} \dfrac{Ldi_L}{dt} = -d \times R_1 i_L - (1-d) \times R_2 i_L - (1-d) \times \dfrac{Rv_C}{r_C + R} - (1-d) \times V_D + dv_{in} \\ \dfrac{Cdv_C}{dt} = (1-d)\dfrac{Ri_L}{r_C + R} - \dfrac{v_C}{r_C + R} \end{cases} \tag{3. 55}$$

where $R_1 = r_{in} + r_{ds} + r_L$ and $R_2 = r_L + r_d + \frac{r_C}{r_C + R}$

The steady state currents and voltages can be calculated using this average system. To produce steady-state currents and voltages, zero must replace the left-hand side. The steady state values are denoted by capital letters. I_L, for instance, indicates the steady-state inductor current:

$$\begin{cases} 0 = -(DR_1 + (1-D)R_2)I_L - (1-D) \times \dfrac{RV_C}{r_C + R} - (1-D) \times V_D + DV_{IN} \\ 0 = (1-D)\dfrac{RI_L}{r_C + R} - \dfrac{V_C}{r_C + R} \end{cases} \tag{3. 56}$$

Steady state values are given as:

$$\begin{cases} I_L = \dfrac{(R + r_C)(DV_{IN} - V_D + DV_D)}{RR_2 + R_2 r_C - 2DR^2 + R^2 + D^2R^2 + DRR_1 - DRR_2 + DR_1 r_C - DR_2 r_C} \\ V_C = \dfrac{R(R + r_C)(D-1)(DV_{IN} - V_D + DV_D)}{RR_2 + R_2 r_C - 2DR^2 + R^2 + D^2R^2 + DRR_1 - DRR_2 + DR_1 r_C - DR_2 r_C} \end{cases} \tag{3. 57}$$

The output equation must also be applied to the averaging procedure:

$$\begin{cases} v_O \times d.T = \dfrac{Rv_C}{r_C + R} \times d.T \\ v_O \times (1-d).T = R\left(\dfrac{r_C i_L}{r_C + R} + \dfrac{v_C}{r_C + R}\right) \times (1-d).T \end{cases} \tag{3. 58}$$

The sides that correspond are added together:

$$d.T \times v_O + (1-d).T \times v_O = d.T \times \frac{Rv_C}{r_C + R} + (1-d).T \times R\left(\frac{r_C i_L}{r_C + R} + \frac{v_C}{r_C + R}\right) \tag{3. 59}$$

Multiplying both sides by $\frac{1}{T}$ completes the averaging of the equation set. If we multiply both sides by $\frac{1}{T}$ and perform the basic algebraic operations, we get:

$$v_O = \frac{(1-d)Rr_C i_L}{r_C + R} + \frac{Rv_C}{r_C + R} \tag{3. 60}$$

The state-space average model of buck-boost converter with R-load shown has nonlinear in nature as the control parameter (d) is in matrix A. Therefore, small signal analysis is required to make the state space to be linear.

3.7. Small Signal Model of Buck-Boost Converter

Due to small variation $\tilde{d}$ of in steady state D, the state variables are changed to $I_L + \tilde{i}_L$ and $V_C + \tilde{v}_C$ .Since-switching converters are nonlinear systems, it is desirable to construct ac small signal linearized models to design linear control system. This is accomplished by perturbing and linearizing the state space averaged model around precise operating point[23]. From the ac small signal model, the most important small signal transfer function can be derived.

Systems average equations are obtained as:

$$\begin{cases} \frac{Ldi_L}{dt} = -d \times R_1 i_L - (1-d) \times R_2 i_L - (1-d) \times \frac{Rv_C}{r_C + R} - (1-d) \times V_D + dv_{in} \\ \frac{Cdv_C}{dt} = (1-d)\frac{Ri_L}{r_C + R} - \frac{v_C}{r_C + R} \end{cases} \tag{3. 61}$$

where $R_1 = r_{in} + r_{ds} + r_L$ and $R_2 = r_L + r_d + \frac{r_C}{r_C + R}$

$$i_L = I_L + \tilde{i}_L \tag{3. 62}$$

$$v_C = V_C + \tilde{v}_C \tag{3. 63}$$

$$d = D + \tilde{d} \tag{3. 64}$$

Where $\tilde{i}_L \ll I_L, \tilde{v}_C \ll V_C$ and $\tilde{d} \ll D$ Diode-forward voltage loss across the diode has been considered to remain constant. These equations indicate that each state has a steady state value($I_L, V_C,$ and D) as well as a small perturbation($\tilde{i}_L, \tilde{v}_C$ and $\tilde{d}$). The average system equation is solved with the left-hand side equal to zero (see Eq. (3.57) to yield steady state values.

Then new variables are placed in to equation

$$\begin{cases} \frac{Ld(I_L + \tilde{i}_L)}{dt} = -(D + \tilde{d}) \times R_1(I_L + \tilde{i}_L) - \left(1 - (D + \tilde{d})\right) \times R_2 i_L \\ \qquad - \left(1 - (D + \tilde{d})\right) \times \frac{Rv_C}{r_C + R} - \left(1 - (D + \tilde{d})\right) \times V_D + (D + \tilde{d})v_{in} \end{cases} \tag{3. 65}$$

Performing some basic algebraic operations in Eq (3.65),

$$-DR_1I_L-(1-D)R_2I_L-(1-D)V_D+\frac{(1-D)RV_C}{r_C+R}+DV_{IN}+(R_2(D-1)-DR_1)\tilde{i}_L-\frac{(1-D)R\tilde{v}_C}{r_C+R}+\left(V_{IN}+(R_2-R_1)I_L+V_D+\frac{RV_C}{r_C+R}\right)\tilde{d}+D\tilde{v}_{in}-R_1\tilde{i}_L\tilde{d}+\tilde{d}\tilde{v}_{in}+R_2\tilde{i}_L\tilde{d}+R\tilde{v}_C\tilde{d} \quad (3.66)$$

Since the derivative of a constant term is zero, $\frac{Ld(I_L+\tilde{i}_L)}{dt}=\frac{Ld\tilde{i}_L}{dt}$. The right side can be divided into three categories:

- $-DR_1I_L-(1-D)R_2I_L-(1-D)V_D+\frac{(1-D)RV_C}{r_C+R}+DV_{IN}$
- $-R_1\tilde{i}_L\tilde{d}+\tilde{d}\tilde{v}_{in}+R_2\tilde{i}_L\tilde{d}+R\tilde{v}_C\tilde{d}$
- $(R_2(D-1)-DR_1)\tilde{i}_L-\frac{(1-D)R\tilde{v}_C}{r_C+R}+\left(V_{IN}+(R_2-R_1)I_L+V_D+\frac{RV_C}{r_C+R}\right)\tilde{d}+D\tilde{v}_{in}$

If we insert the steady state values given before Eq. (3.57) in to $-DR_1I_L-(1-D)R_2I_L-(1-D)V_D+\frac{(1-D)RV_C}{r_C+R}+DV_{IN}$ the result will be 0. The second group can be eliminated. Because the product of two small numbers is also a small number. As a result, only the third category is significant:

$$\frac{Ld\tilde{i}_L}{dt}\approx(R_2(D-1)-DR_1)\tilde{i}_L-\frac{(1-D)R\tilde{v}_C}{r_C+R}+\left(V_{IN}+(R_2-R_1)I_L+V_D+\frac{RV_C}{r_C+R}\right)\tilde{d}+D\tilde{v}_{in} \quad (3.67)$$

The capacitor voltage equation can be solved using the same method.

$$\left\{\frac{Cd(V_C+\tilde{v}_C)}{dt}=\left(1-(D+\tilde{d})\right)\frac{R(I_L+\tilde{i}_L)}{r_C+R}-\frac{(V_C+\tilde{v}_C)}{r_C+R}\right. \quad (3.68)$$

Because V C is constant, its derivative is also zero. So,

$$\frac{Cd(V_C-\tilde{v}_C)}{dt}=\frac{(1-D)RI_L}{r_C+R}-\frac{V_C}{r_C+R}+\frac{(1-D)R\tilde{i}_L}{r_C+R}-\frac{\tilde{v}_C}{r_C+R}-\frac{RI_L\tilde{d}}{r_C+R}-\frac{R\tilde{i}_L\tilde{d}}{r_C+R} \quad (3.69)$$

The right side can be divided into three categories:

- $\frac{(1-D)RI_L}{r_C+R} - \frac{V_C}{r_C+R}$
- $-\frac{R\tilde{i}_L\tilde{d}}{r_C+R}$
- $\frac{(1-D)R\tilde{i}_L}{r_C+R} - \frac{\tilde{v}_C}{r_C+R} - \frac{RI_L\tilde{d}}{r_C+R}$

If we insert the steady state values given before Eq. (3.57) in to $-DR_1I_L - (1-D)R_2I_L - (1-D)V_D + \frac{(1-D)RV_C}{r_C+R} + DV_{IN}$ the result of will be 0. The second group can also be eliminated. Because the product of two small numbers is also a small number. As a result, only the third category is significant:

$$\frac{C(d\tilde{v}_C)}{dt} \approx \frac{(1-D)R\tilde{i}_L}{r_C+R} - \frac{\tilde{v}_C}{r_C+R} - \frac{RI_L\tilde{d}}{r_C+R} \tag{3. 70}$$

In the same way, the output equation is linearized. The output voltage (v_O) is split into two parts:

- Large signal component (V_O) and
- Small signal component ($\tilde{v}_O$).

In the averaged equation (Eq. 3.60), we replace variables with their respective large and small signal parts:

$$V_O + \tilde{v}_O = \frac{\left(1-\left(D+\tilde{d}\right)\right)Rr_C(I_L+\tilde{i}_L)}{r_C+R} + \frac{R(V_C+\tilde{v}_C)}{r_C+R} \tag{3. 71}$$

Applying some basic algebraic operations:

$$V_O + \tilde{v}_O = \frac{(1-D)Rr_CI_L}{r_C+R} + \frac{RV_C}{r_C+R} + \frac{(1-D)Rr_C\tilde{i}_L}{r_C+R} + \frac{R\tilde{v}_C}{r_C+R} - \frac{Rr_CI_L\tilde{d}}{r_C+R} - \frac{Rr_C\tilde{i}_L\tilde{d}}{r_C+R} \tag{3. 72}$$

The large signal component of the output can be calculated as follows:

$$V_O = \frac{(1-D)Rr_CI_L}{r_C+R} + \frac{RV_C}{r_C+R} \tag{3. 73}$$

The output steady state value is obtained by substituting the steady state values for I L and V C (Eq. (3.56)) into (3.71).

We are considered in the small signal component. So, only the small signal terms are considered:

$$\tilde{v}_O = \frac{(1-D)Rr_C\tilde{i}_L}{r_C+R} + \frac{R\tilde{v}_C}{r_C+R} - \frac{Rr_CI_L\tilde{d}}{r_C+R} \tag{3. 74}$$

As a result, the Buck converter's linearized small signal model can be stated as:

$$\begin{cases} \frac{d\tilde{i}_L}{dt} \approx \frac{1}{L}\left[(R_2(D-1)-DR_1)\tilde{i}_L - \frac{(1-D)R\tilde{v}_C}{r_C+R} + \left(V_{IN} + (R_2-R_1)I_L + V_D + \frac{RV_C}{r_C+R}\right)\tilde{d} + D\tilde{v}_{in}\right] \\ \frac{(d\tilde{v}_C)}{dt} \approx \frac{1}{C}\left[\frac{(1-D)R\tilde{i}_L}{r_C+R} - \frac{\tilde{v}_C}{r_C+R} - \frac{RI_L\tilde{d}}{r_C+R}\right] \end{cases} \tag{3. 75}$$

$$\tilde{v}_O = \frac{(1-D)Rr_C\tilde{i}_L}{r_C+R} + \frac{R\tilde{v}_C}{r_C+R} - \frac{Rr_CI_L\tilde{d}}{r_C+R} \tag{3. 76}$$

where $R_1 = r_{in} + r_{ds} + r_L$ and $R_2 = r_L + r_d + \frac{r_C}{r_C+R}$

It can be expressed as a state space equation, as follows:

$$\begin{cases} \dot{x} = Ax + Bu \\ y = Cx + Du \end{cases} \tag{3. 77}$$

where

$$x = \begin{bmatrix} \tilde{i}_L \\ \tilde{v}_C \end{bmatrix},$$

$$u = \begin{bmatrix} \tilde{d} \\ \tilde{v}_{in} \end{bmatrix},$$

$$y = u_O,$$

$$A = \begin{bmatrix} \frac{(R_2(D-1)-DR_1)}{L} & -\frac{(1-D)R}{(r_C+R)L} \\ \frac{(1-D)R}{(r_C+R)C} & -\frac{1}{(r_C+R)C} \end{bmatrix} \tag{3. 78}$$

$$B = \begin{bmatrix} \frac{1}{L}\left(V_{IN} + (R_2-R_1)I_L + V_D + \frac{RV_C}{r_C+R}\right) & \frac{D}{L} \\ \frac{RI_L}{C(r_C+R)} & 0 \end{bmatrix},$$

$$C = \begin{bmatrix} \frac{(1-D)Rr_C}{r_C+R} & \frac{R}{r_C+R} \end{bmatrix},$$

$$D = \begin{bmatrix} -\frac{Rr_C I_L}{r_C + R} & 0 \end{bmatrix}$$

Again, equate ac and dc variables and proceed with ac equations by ignoring second order ac quantities (remove the product of any ac terms because they are nonlinear, as they involve the multiplication of time-varying signals, and they are considerably smaller than first-order ac terms) produces:

The Laplace transform of equation (3.78) produces the following:

$$\mathrm{S(S)\tilde{i}_L(S) = (R_2(D-1) - DR_1)\tilde{i}_L(S) - \frac{(1-D)R\tilde{v}_C(S)}{r_C + R} + \left(V_{IN} + (R_2 - R_1)I_L + V_D + \frac{RV_C}{r_C + R}\right)\tilde{d}(S) + D\tilde{v}_{in}} \quad (3.\ 79)$$

$$\mathrm{CS\tilde{v}_C\ (s) = \frac{(1-D)R\tilde{i}_L(S)}{r_C + R} - \frac{\tilde{v}_C(S)}{r_C + R} - \frac{RI_L\tilde{d}(S)}{r_C + R}}$$

$$\mathrm{\tilde{v}_O(S) = \frac{(1-D)Rr_C\tilde{i}_L(S)}{r_C + R} + \frac{R\tilde{v}_C(S)}{r_C + R} - \frac{Rr_C I_L\tilde{d}(S)}{r_C + R}} \quad (3.\ 80)$$

Variation in output voltage with variation in input voltage and converter transfer function with controlled duty ratio is the most important. As a result, make $\mathrm{\tilde{d}(S) = 0}$ to obtain the transfer function from the input voltage to the output voltage, and make $\mathrm{\tilde{v}_{in}(S) = 0}$ to obtain the transfer function from the duty ratio to the output voltage. Variation in input voltage act as a disturbance, and the converter is regulated by the duty ratio of the input pulse.

The buck-boost converter is rated for a resistive load of 40 watts. Because the load voltage is set to 24 V and the load current is calculated to be 1.67 A, the load resistance of 14.4 is calculated according to ohm's law. After setting all of these parameters, the input voltage for a buck-boost converter is set to 12 V, because the input voltage must be lower than the output voltage (24 V) and buck-boost converter designed for LED light bulb.

Table 3.1: Parameters of buck-boost converter system

No.	Description	Parameter	Value	Unit
1	Input voltage	V_{in}	12	V
2	Output voltage required	V_o	24	V
3	Capacitance	C	16.44	μF
4	Inductance	L	78.41	μH
5	Load resistance	R	14.4	Ω
6	Switching frequency	F	100	KHz
7	Duty cycle	D	0.67	-

The transfer function of buck-boost converter Equation (3.80) is simplified and obtained using Matlab code by using parameters value given.

The small signal transfer functions for the given values are described as:

$$\frac{\tilde{v}_O(s)}{\tilde{d}(s)} = \frac{-0.2099s^2 - 2.492 \times 10^5 + 7.475 \times 10^9}{s^2 + 7440s + 9.903 \times 10^7} \quad (3.\ 81)$$

$$\frac{\tilde{v}_O(s)}{\tilde{v}in(s)} = \frac{141.1s + 1.717 \times 10^8}{s^2 + 7440s + 9.903 \times 10^7} \quad (3.\ 82)$$

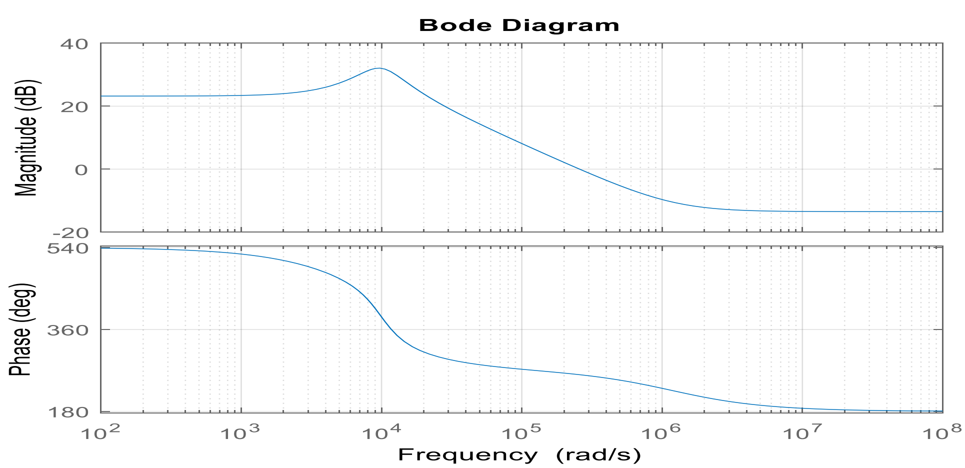

Figure 3.8 Bode plot of transfer function of output with duty ratio for a Buck-boost converter

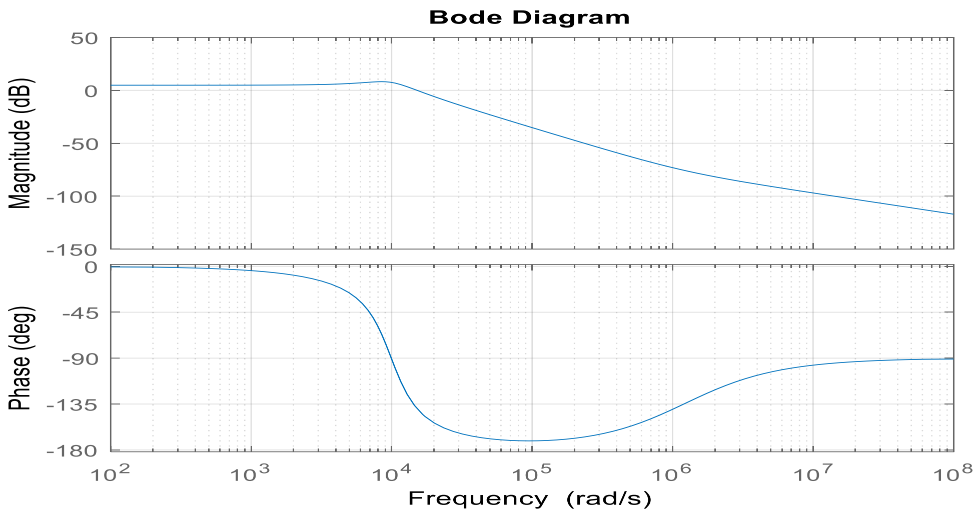

Figure 3.9: Bode plot of transfer of output with input change for a Buck-Boost converter

3.8. Effect of Parasitic Elements on the Performance of Buck-Boost Converter

In buck-boost converter, inductor, capacitor and MOSFET switch is used. In all these, there are parasitic elements which affect the performance of buck-boost converter. Due to parasitic elements voltage gain reduces and this gain reduction is avoided by limiting the duty ratio. Due to parasitic element up to certain value of duty ratio the gain increases after that gain reduces drastically

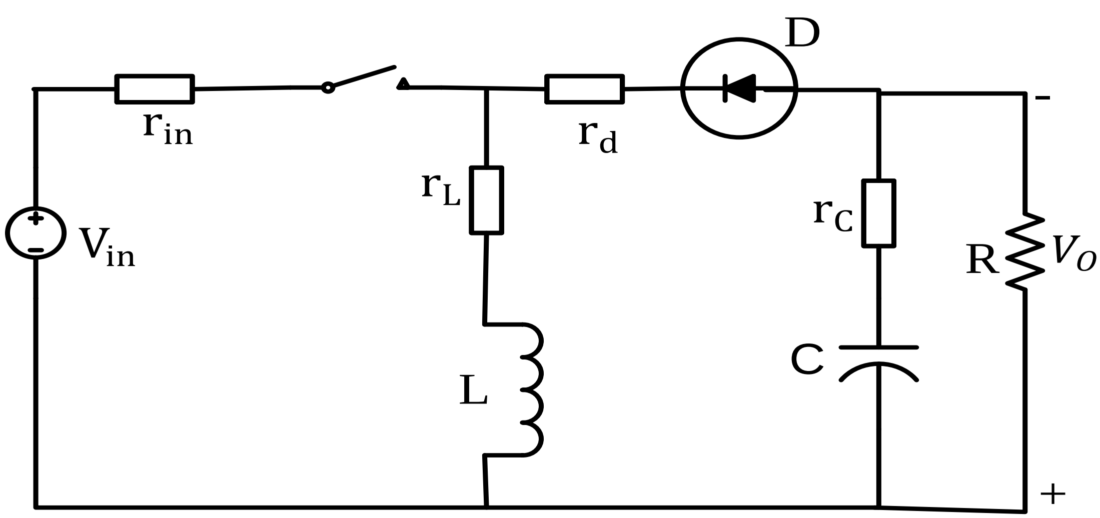

Figure 3.10: Buck-Boost converter with effect of parasitic resistance

Effect of Parasitic Element in Mosfet: The MOSFET device is connected in parallel with an internal diode that turns on when the MOSFET device is reverse biased. This internal diode is provided to protect against reverse voltage. The model is done using an ideal switch and it is turned ON or OFF using a gate signal g. The diode is connected in parallel with the switch:

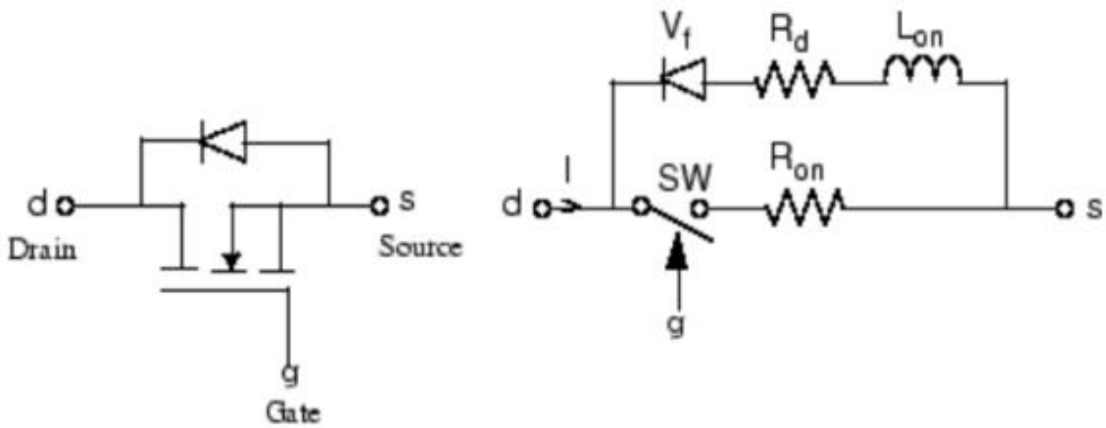

Figure 3.11: MOSFET and its equivalent circuit

The ON state voltage of MOSFET Vds will vary according to the following:

- When MOSFET is turned ON Vds=Rds(on)* I, where I is the current flowing through the device when it is turned ON.
- When the device is turned OFF, anti-parallel diode starts conducting then;

Vds = Rd*I-Vf +Lon*di/dt where Vf is the internal diode forward voltage drop. The anti-parallel diode inductance is denoted as Lon and it is used only for continuous systems. For discrete systems this has been set to zero. The initial current is denoted as Ic and it is the initial value of current that flows in the MOSFET.

3.9. Equilibrium points and stability analysis

3.9.1. Review on Equilibrium Points

- ❖ Consider a nonlinear state space model given by:

$$x(t) = f[t,x(t)],t\geq 0$$

- ❖ A vector x_o is called an equilibrium if:

$$f(t,x_0) = 0,\forall t\geq 0$$

- ❖ Equilibrium points are solutions of the differential equation and each solution point determines an equilibrium point.[24]

From buck-boost state space equation we have the following:

$$\left.\begin{aligned} \dot{x}_1 &= \frac{-1}{RC}x_1 + (d-1)\frac{-1}{C}x_2 \\ \dot{x}_2 &= \frac{(d-1)}{L}x_1 + \frac{d}{L}u(t) \end{aligned}\right\} \tag{3. 83}$$

Where X_1 is output voltage and X_2 is output inductor current of the buck-boost converter.

Again, from equation (3.81) let $\dot{x}_1 = f_1$ and $\dot{x}_2 = f_2$, and let be $f_1, f_2 = 0$ then we have

$$\left.\begin{aligned} &\frac{-1}{RC}x_1 + (d-1)\frac{-1}{C}x_2 = 0 \qquad * \\ &\frac{(d-1)}{L}x_1 + \frac{d}{L}u(t) = 0 \qquad ** \end{aligned}\right\} \tag{3. 84}$$

From equation (3.84) of (**) solving for x_1:

$$x_1 = -\frac{d}{(d-1)}u(t) \tag{3. 85}$$

Inserting equation (3.85) in to equation (3.84) of (*) and solving for x_2:

$$x_2 = -\frac{d}{R(d-1)^2}u(t) \tag{3. 86}$$

Therefore, the equilibrium points are given as:

$$\left.\begin{aligned} x_1 &= -\frac{d}{(d-1)}u(t) \\ x_2 &= -\frac{d}{R(d-1)^2}u(t) \end{aligned}\right\} \tag{3. 87}$$

From equation (3.85), we can see that the equilibrium point of the buck-boost converter depends on the input and it exhibits bifurcation property. Substituting the value of parameters from appendix A, we can get the value of x_1 and x_2.i.e. $x_1 = 24.36$ and $x_2 = 5.13$. The types of equilibrium point of the system are determined by calculating the pole of the transfer function of the system. Therefore, the pole of $\frac{\tilde{v}_O(s)}{\tilde{d}(s)}$ will be:

poles ($\frac{\tilde{v}_O(s)}{\tilde{d}(s)}$) = 1.0e+03 *

-4.6414 + 9.1202i

-4.6414 - 9.1202i

From the result both poles are complex and their real part is less than zero; in this condition the type of equilibrium point stability is called stable focus.

3.9.2. Review and checking stability of nonlinear system

Stability in nonlinear systems is defined based on the equilibrium points. An equilibrium point is stable if a solution starting from an initial state inside a ball of small radius should remain inside a small radius for all time. An equilibrium point is unstable if it is not stable, this can be in any one of the following ways[24]

- The system trajectory goes to infinity starting from an initial condition.
- The solution trajectory goes far from the equilibrium point.
- The system trajectory forms a limit cycle.

3.9.3. Local stability analysis using Lyapunov direct method.

There are two main steps of checking local stability using Lyapunov /direct method. Step 1: The first step is choosing positive definite lyapunov candidate function

Definition: - Let V (lyapunov function) be a continuous map from R^n to R. We call V (x) a locally positive definite (lpd) function around x = x_0 (equilibrium point) if:

a. V(x_0) = 0
b. V(x_0) > 0, 0<||x||<r, for some r[24].

Step 2: Then the second step is checking lyapunov function derivative along state trajectories around an equilibrium point.

Theorem 1: If there exists a lyapunov function of a system V(x), then x = x_0 point in the sense of lyapunov, if in addition $\dot{V}(x_0)$ > 0, 0<||x||<r, for some r. Then x = x_0 is an asymptotically stable Equilibrium point[24].

To check the stability of equilibrium points of the buck-boost converter using lyapunov direct method by choosing lyapunov function, positive definite function: V = $\frac{1}{2}{x_1}^2 + \frac{1}{2}{x_2}^2$ (Positive definite function),Then computing derivative of Lyapunov function $\dot{V}$ = $x_1\dot{x_1} + x_2\dot{x_2},$ evaluating

$\dot{V}$ around an equilibrium points $\dot{V} < 0$, so the equilibrium points in x direction exhibit stable behavior.

The result from Fig. (3.12) shows the states (x= x_1, x_2 and y= $\dot{x}_1, \dot{x}_2$) starts initially at [0, 0.01] point and goes away to [40, 20] point after 10 elapsed seconds. The initial point is far from the equilibrium point [24.36, 5.13] but it stays around the equilibrium point after 10 seconds or it moves to the equilibrium point from the initial condition. This indicate the equilibrium point exhibits stable behavior.

3.10 Controller Design

The controller was introduced to the control system, causing the output to follow the input more quickly and reducing the error value. For buck-boost converter some linear and nonlinear controller are applied and their performance are stated in this paper.

Changes in input voltage act as a disturbance, and the converter is controlled by the duty ratio of the input pulse. Block diagram of buck-boost converter with controller and without controller is given[22]:

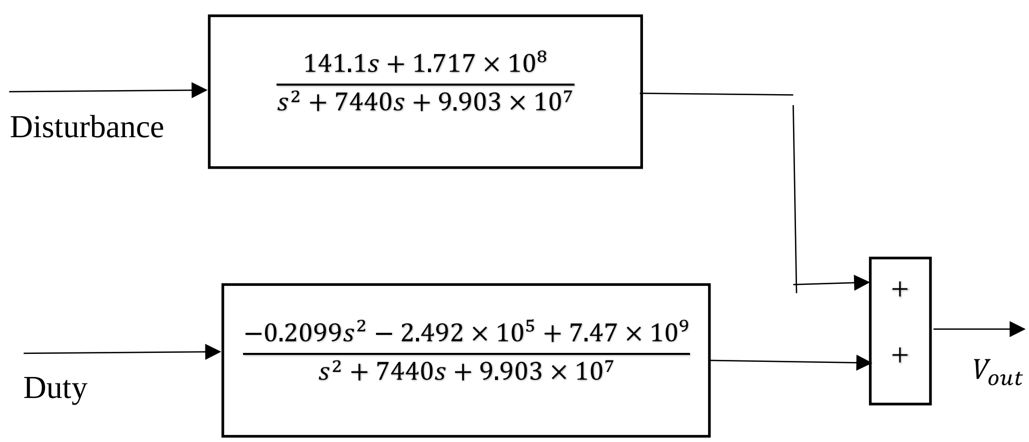

Figure 3.12: open loop of a Buck-boost converter.

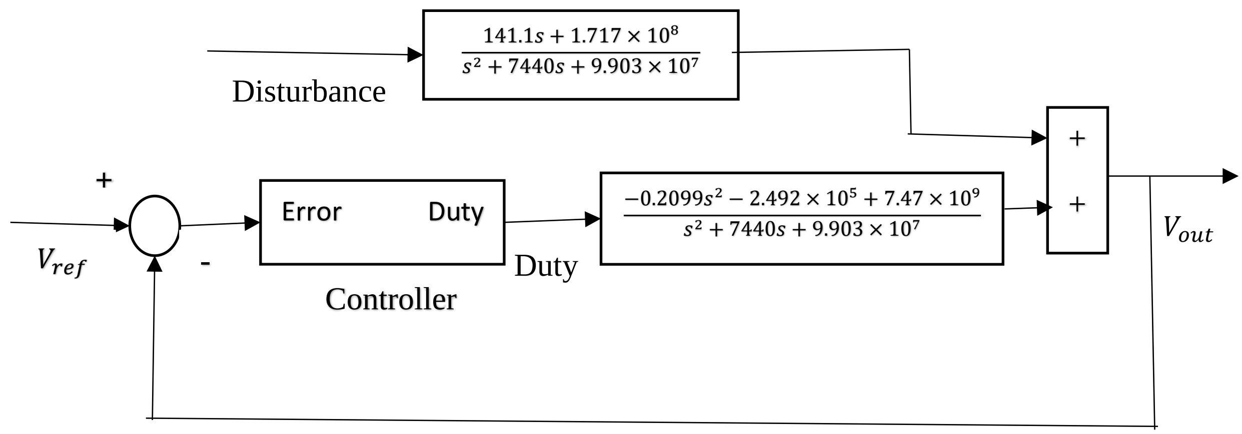

Figure 3.13: Closed loop of a Buck-boost converter.

The controller in this block diagram senses the difference between the references and sets the duty based on the difference. Because the feedback is obtained from the output voltage, this is known as Voltage Mode Control (VMC) [22].

3.10.1 PI Controller for Buck Boost Converter

Because of its capacity to compensate for most practical industrial processes, the PI controller has been used in many industrial applications. PI and PID controllers are used to control most low to medium order processes. Over 85% of control loops are regulated by a single input and output, which has led to the development of PI and PID controllers [5].

Pi controller for buck-boost converter in this case designed by using transfer function given and pi tuner command is used to tune the Pi controller coefficient. Block diagram of Pi controller for buck boost converter system shown as:

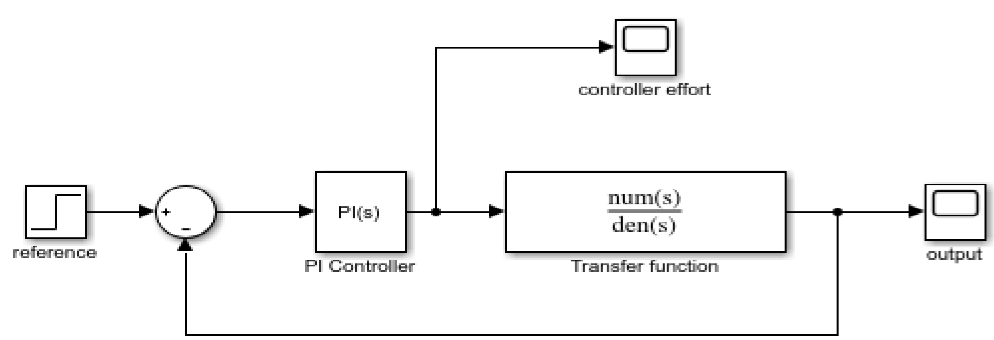

Figure 3.14 Pi Controller buck boost converter

After trial and error are finished Pi controller gains for this system are obtained. By applying this technique the value Kp=0.00144 and Ki=22.26. Performance of this controller is discussed in next chapter.

3.10.2 PID Controller for Buck Boost Converter

Since the 1980s, process automation technology has advanced significantly. The processing power of controllers, in particular, has increased dramatically, influencing the types of controls employed in applications. Most controllers employed single-loops and a single-variable in the past. Multi-loop and multi-variable controllers are now widely employed in a variety of applications[5]. The PID controller serves as the foundation for these control schemes. A proportional element, an integral element, and a derivative element make up this system. Because the gain constants are initialized at the start and then kept constant throughout the operation, the PID controller is inefficient when the surrounding environment changes. Figure 3.16 shows a PID controller block diagram in any system with all three PID components connected in parallel. Kp, Ki, and Kd represent the gains of P, I, and D elements, respectively. The error sigma is used as a PID controller's input.

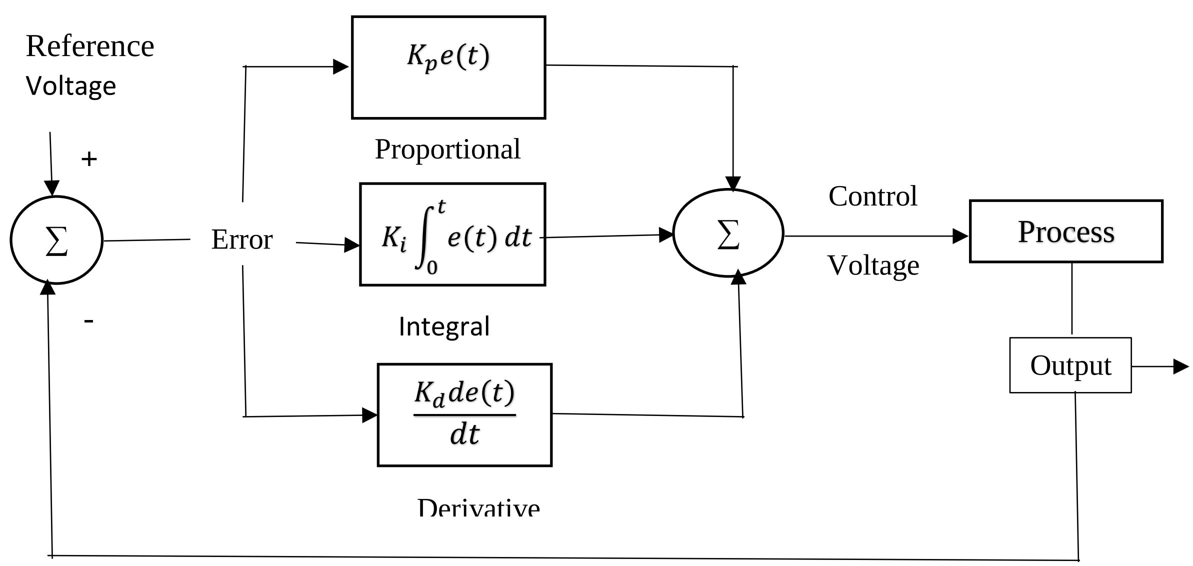

Figure 3.15 Block Diagram of a PID Controller

The PID controller's output is as follows:

$$U(t) = K_p e(t) + K_i \int_0^t e(t)dt + \frac{K_d de(t)}{dt} \tag{3.88}$$

Its transfer function is defined as:

$$C(s) = \frac{U(s)}{E(s)} = K_p + \frac{K_i}{s} + K_d s = K_p(1 + \frac{1}{sT_i} + sT_d) \tag{3.89}$$

Kp, Ki, and Kd are the proportional, integral, and differential gains, respectively and constant $T_i = \frac{K_p}{K_i}$ and $T_d = \frac{K_d}{K_p}$

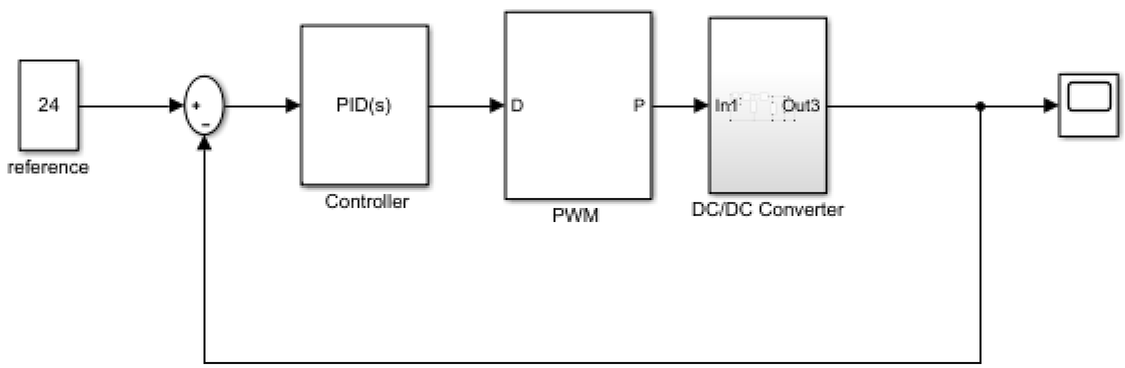

Figure 3.16 The PID controller for Buck-Boost converter

The control signal enters the pulse width modulation and affects the length of time the switch is switched during a switching cycle. The control signal's level is theoretically limited between zero and one, as symbolized by the limiter in the buck-boost converter's schematic circuit. This limitation introduces a new non-linearity that was not taken into account when the mathematical model and transfer function of the system were developed.

The system will become insensitive to further changes in the error signal if the level of the control signal exceeds the limiter's range. As a result, we must use extra care when determining the controller's parameters. Because the controlling signal does not exceed one, we will use the inverse of the reference voltage for the maximum allowed proportional gain[6]:

$$K_{pmax} = \frac{1}{V_{ref}} \quad (3.90)$$

In steady state, we multiply the allowable gain K_{pmax} by the factor d to get the maximum critical gain. In the case of a buck-boost converter, the critical period of oscillations T_{cr} is obtained by measuring the period of oscillations related to the maximal allowed proportional gainK_{pmax}. The minimum oscillatory period can be measured at all and corresponds to undamped oscillations of the output. For the purposes of PID tuning, it will be assumed that this time approximates the system critical period with high accuracy[25].

$$T_{cr} = 2\pi\sqrt{LC} \quad (3.91)$$

Using the adopted K_{cr} i T_{cr} values and Ziegle-Nichols guidelines for PID tuning without overshoot, unknown PID controller parameters could be evaluated as follows[6]:

$$K_p = 0.2\frac{d}{V_{ref}} \quad K_i = \frac{2K_p}{T_{cr}} \qquad K_d = \frac{K_p T_{cr}}{3} \quad (3.92)$$

PID controller gains are determined as follow by using buck-boost converter specification given:

$$K_p = 0.2\frac{d}{V_{ref}} = 0.006 \text{ , } T_{cr} = 2\pi\sqrt{LC} = 0.0002, K_i = \frac{2K_p}{T_{cr}} = 5.371, K_d = \frac{K_p T_{cr}}{3} = 4.55 * 10^{-7}$$

After applying PID controller gains to buck-boost converter closed loop unit step response of the system performance is evaluated using Matlab Simulink.

3.10.3 GA-PID controller

The Genetic Algorithm solves optimization problems by employing techniques that are based on natural evolution, such as inheritance, selection, crossover, and mutation**.** The controller parameters are tuned to generate appropriate transient response without affecting the steady operation using the GENETIC ALGORITHM, which is an adaptive method for solving search and optimization problems.

Structure of GA-Proportional Integral Derivative (PID) Controller

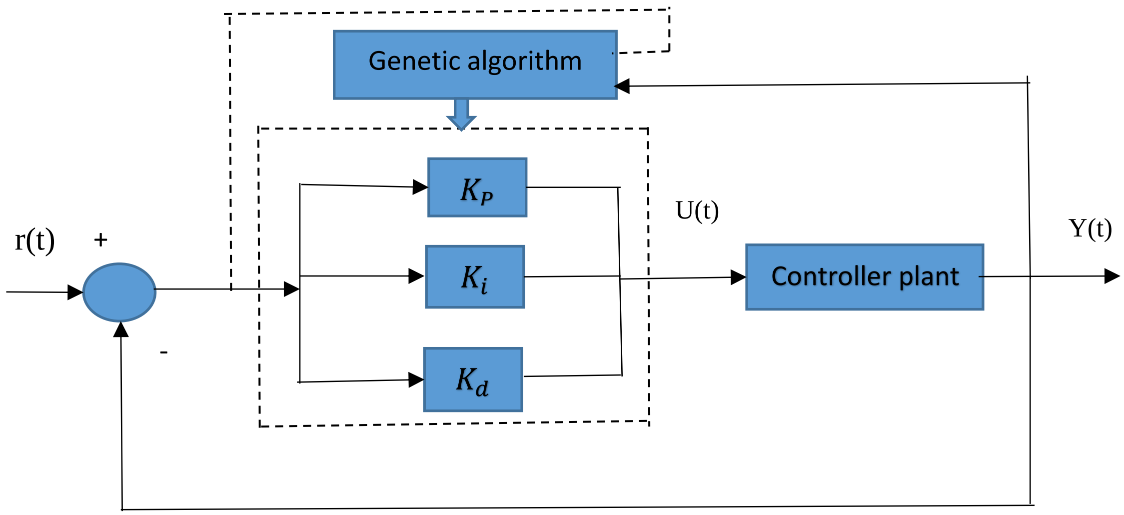

Figure 3.17 Structure of GA-PID Controller[26]

This section explains how GA –PID controller is designed and implemented. The following are the steps in order:

Step1: Create a population of initial solution of parameters $\phi = \{K_p, K_i$ and K_d}

Step 2: Evaluation of fitness function

A solution's degree of "goodness" is determined by assigning a value to it. This is accomplished by assigning the problem a correct fitness function. The following is the fitness function[27]:

$$\text{Fitness function} = \frac{1}{1+F(\phi)}$$

Step 3: Generation of offspring

Selection, crossover, and mutation are all involved.

Step4: Replace the current population with the new population

Step5: Terminate the program if termination reached; else go to step 2.

The GA based PID controller for dc-dc buck boost converter is implemented. The details of the GA optimization parameters setting used in simulation for tuning of PID controller of dc-dc buck-boost converter are shown below in table 3.2.

Table 3.2. Parameter setting of the genetic optimization

Parameter	type and value
Maximum generation	20
Population size	30
Selection	Uniform
Mutation	Uniform
Crossover	single point Crossover
No. of parameters	3
Lower boundary	[0.0013 15 1e-8]
Upper boundary	[0.0014 23 1e-7]

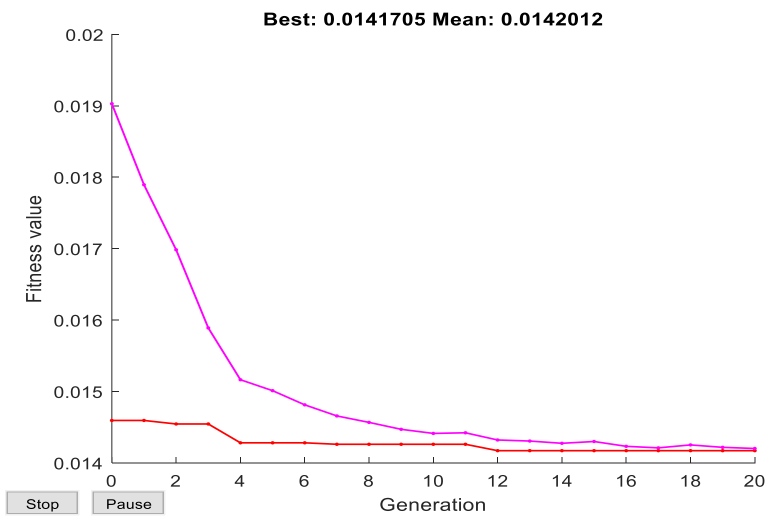

Figure 3.18 The convergence characteristic curve.

The model of dc-dc buck- boost converter for voltage control of PID is performed in GA optimization. The parameters of the dc-dc buck- boost converter for voltage control with GA based PID controller gain (Kp, Ki, Kd) are obtained as shown in table 3.3

Table 3.3 the GA optimized parameters of PID controller

Controller	Optimized parameters	Optimized value
PID	Kp	0.00135
	Ki	22.869
	Kd	3.356e-08

Using above listed steps GA-PID controller is implemented on buck-boost for voltage control performance of this controller is discussed on next chapter.

3.10.4 Fuzzy Logic Controller.

Fuzzy logic is an artificial intelligence branch that deals with reasoning algorithms that are used to emulate human mind and make computer choices. A grade or level is given a maximum value of 1 and a lowest value of 0 when paired with an information spectrum. Unlike Boolean logic, which specifies that any variable's value must be either 0 or 1, fuzzy logic allows for states in between, such as membership value. In linguistic terms, the grade of membership value of a fuzzy variable can be characterized [28]. The use of language variables rather than numerical variables is one of the main characteristics of the fuzzy primary features.

There are no established techniques for designing fuzzy logic controllers, such as root locus, Nyquist plots, pole positioning, stability checks, and so on. The most difficult component of constructing the procedures is that the rule base has no mathematical description[24].

The rules formed by the Linguistic variables are primarily responsible for fuzzy logic control. Unlike other approaches, fuzzy logic control does not require complicated numerical calculations. The model is regulated solely by simple mathematical calculations. Despite the fact that it relies on simple mathematical analysis, it performs well in a control system. As a result, this method is one of the most effective and simple ways to control a plant. Linguistic variables are variables whose values are defined in a common language (for example, big and small), and which can be represented by a fuzzy set. The general architecture of the FLC controller as shown below.

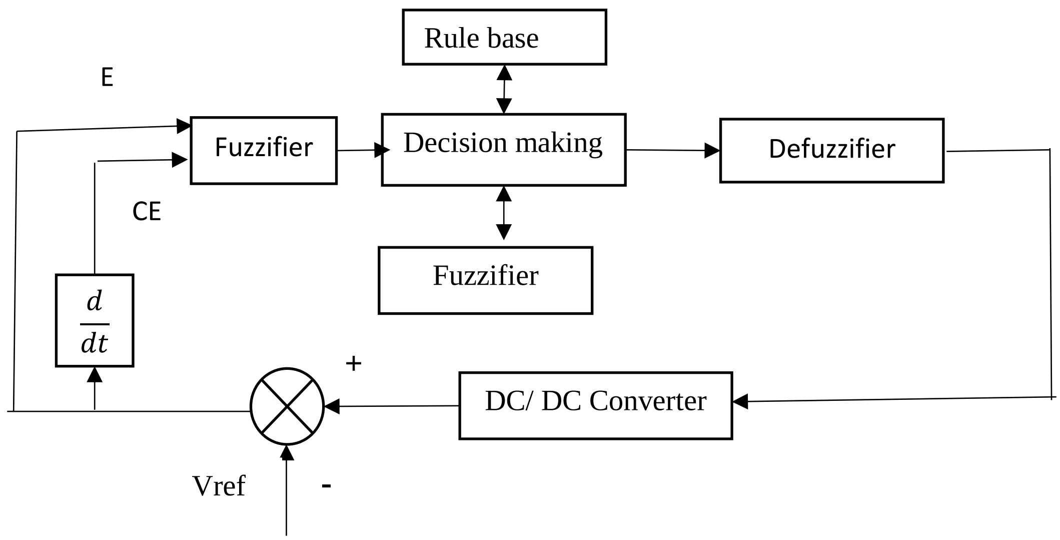

Figure 3.19: Basic Configuration of FLC

Fuzzy logic controller have four basic components:

- **Fuzzifier:** Input data is converted into linguistic values using a fuzzification interface
- **Rule Base and Data Base:** Both are referred to as a knowledge base. It is composed of a database with all of the essential linguistic definitions and a set of control rules.
- **Decision Making:** The fuzzy control action is inferred from knowledge of the control rules and the linguistic variable definition, simulating a human decision process.
- **Defuzzifier:** From an inferred fuzzy control action, a defuzzification interface produces a non-fuzzy control action.

The error E and the change of error CE are the fuzzy logic controller's inputs, which are defined as:

$$e = v_O - v_{ref} \tag{3. 93}$$

$$ce = e_k - v_{k-1} \tag{3. 94}$$

Where Vo is the current output voltage, Vref is the reference input voltage, and k denotes the values taken at the start of the kt switching cycle[29]. The duty cycle is the fuzzy controller's output, and it is defined as follows:

$$d_k = d_{k-1} + h\Delta d_k \tag{3. 95}$$

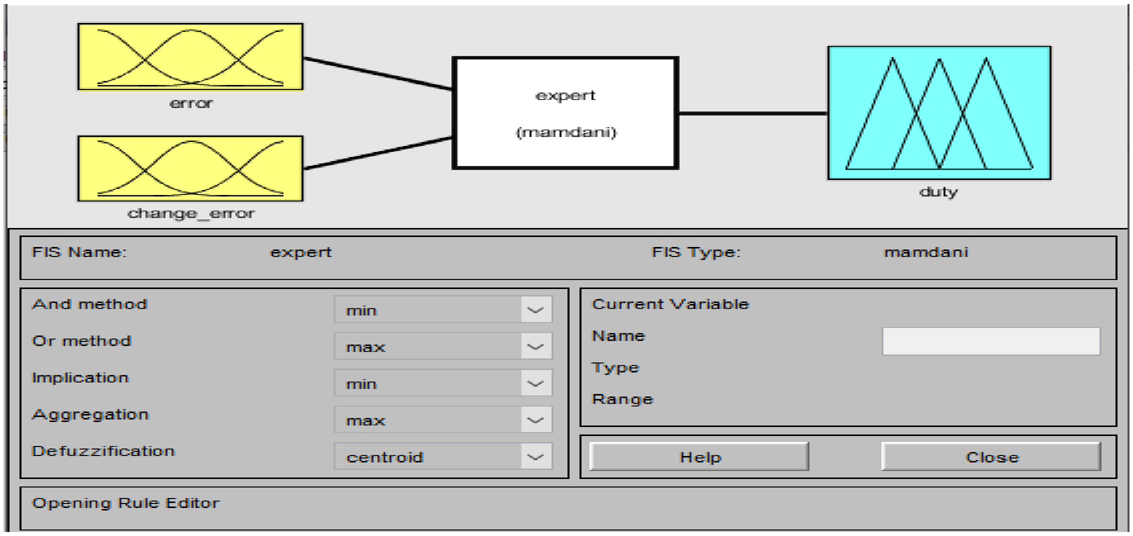

Figure 3.20: The Editor of Fuzzy Inference System using Matlab

As shown in figure 3.20, the fuzzy logic control for DC-DC buck-boost converter is made up of two input variables and one output variable, which are the error and change of error as input variables and the change of duty cycle as an output variable. Five partitions have been created for each control variable. These partitions, known as membership functions, are divided into five fuzzily defined subsets: PB (Positive Big), PS (Positive Small), ZO (Zero), NS (Negative Small), and NB (Negative Big) are all positive terms (Negative Big). Figure 3.20 shows the partitioning of fuzzy subsets and the shape of the membership function, i.e. (error variable) and (change of error variable), and figure 3.21 shows the shape of the membership function (output variable). The triangular forms of this arrangement's membership function indicate that there is only one dominant fuzzy subset for each given input. Table 3.2 lists the rules for the fuzzy regulated buck-boost converter. The fuzzy rule basis is constructed into 25 rules using the tabulated table

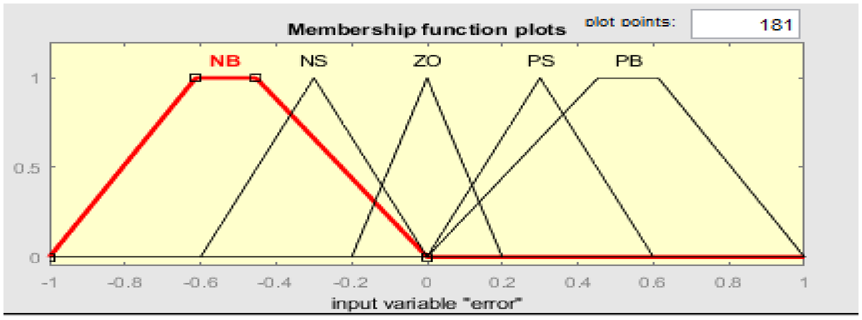

Figure 3.21: Membership Function of Input Variable ‘error

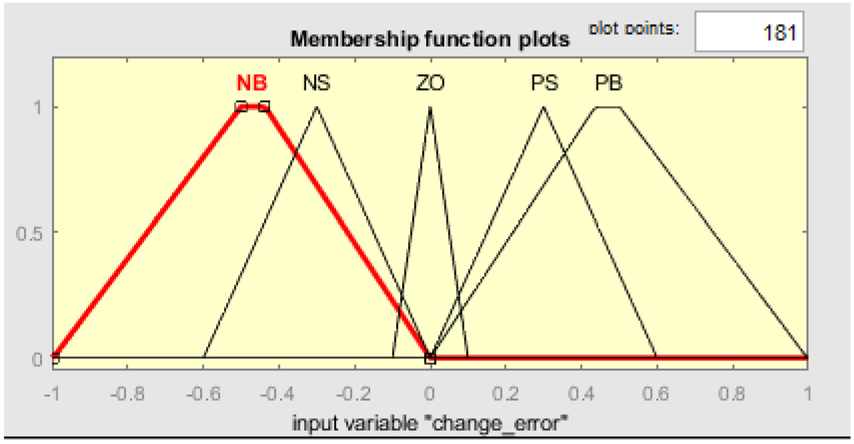

Figure 3.22: Membership Function of Input Variable ‘change of error’

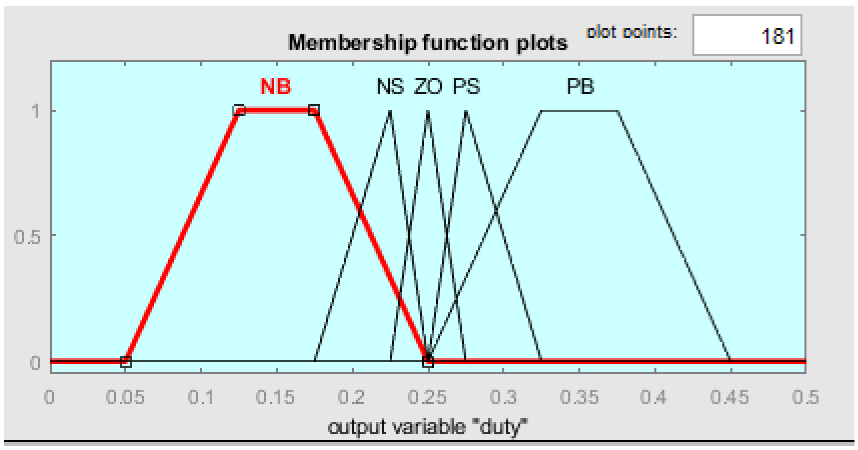

Figure 3.23: Membership Function of Output Variable

Following the construction of the membership functions, the fuzzy controller's rules must be written. These rules are based on the expertise and experience.

Table 3.4: The Rule Base with 25 Rules

		ERROR				
		NB	NS	ZO	PS	PB
CHANGE ERROR	NB	NB	NB	NB	NS	ZO
	NS	NB	NB	NS	ZO	PS
	ZO	NB	NS	ZO	PS	PB
	PS	NS	ZO	PS	PB	PB
	PB	ZO	PS	PB	PB	PB

The surface of a fuzzy controller applying the previous rules is shown in Figure 3.24.Using the Centroid defuzzification, the surface shows the relationship between the inputs and outputs at any point in the intervals [-1 1].

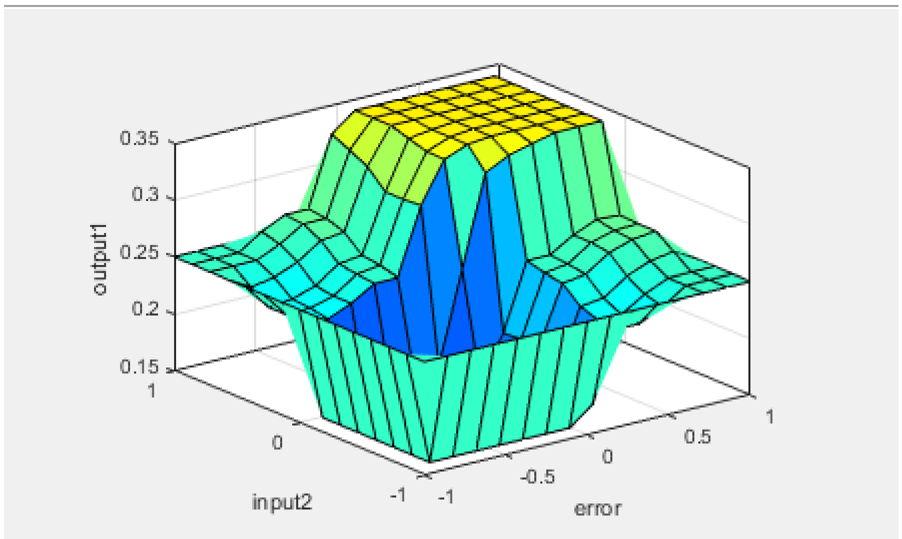

Figure 3.24: Surface of Fuzzy Controller

Figure 3.25 shows the simulation conducted with the Matlab-Simulink environment. Adjusting the duty cycles with respect to the voltage reference of 24V yields the results.

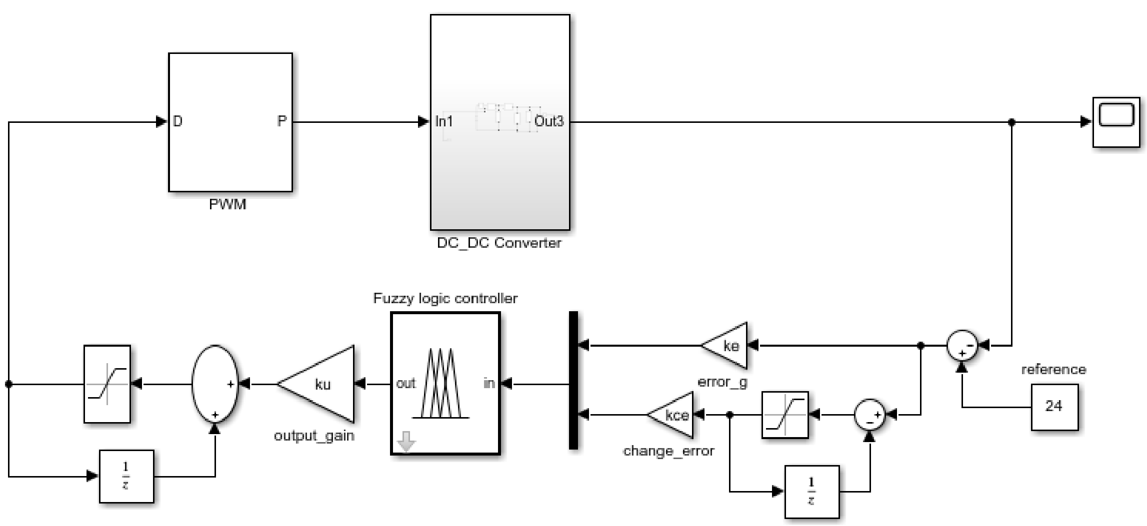

Figure 3.25: Matlab/Simulink Model (buck-boost Converter Closed Loop with Fuzzy Controller)

3.10.5 Fuzzy Controller with GA for Buck-boost DC-DC Converter

In addition to the shape of the memberships of the inputs and outputs of the fuzzy controller, there are several factors that affect the control process of the Buck DC-DC converter model: change of error gain, error gain and output gain (fuzzy output gain). These gain parameters can be tuned to get close to optimal results. GA is used to optimize these parameters as well as the shape of fuzzy controller memberships. There are several strategies to get a good response. The first is to adjust gain parameters only without changing the form of the memberships. The second step is to improve the form of the memberships without changing the gain parameters. The final option is to optimize both the gain parameters and the shape of the memberships. The GA Matlab code (Appendix A) is used to optimize the shape and gain parameters of the memberships. There are two inputs and one output in fuzzy controllers. There are five membership functions for each input and output, three of which are triangular memberships while the others are trapezoidal membership functions.

However, several simplifications are made in the writing of GA code in this thesis.

1-The input intervals will remain in the [-1 1] and output in [0 0.5] range.

2- The symmetric point will remain at a value of zero.

3- The inputs and outputs will be identical in shape.

The number of variables will be five for membership functions and three for gain parameters after this simplification. The integral of the absolute values of the error will be used as the fitness function, and the fitness value must be minimized in the control design. The number of individuals in each population will be 40, the number of generations will be 30, and crossover will be single point Crossover. The model of dc-dc buck- boost converter for voltage control of fuzzy is performed in GA optimization. The parameters of the dc-dc buck-boost converter for voltage control with GA based fuzzy controller gain (ke, kce, ku) are obtained as shown in table 3.5

Table 3.5 the GA optimized gain of fuzzy controller

Controller	Optimized gain	Optimized value
GA-fuzzy	Ke	1.576
	Kce	3.805
	Ku	7.547

3.10.6 Sliding Mode Controller

Sliding mode control (SMC) is a form of Variable Structure Control (VSC) whose main goal is to attract system states to a surface known as the sliding surface. Sliding mode control is a variation on the on-off switch. When the machine answer deviates from the desired actions, the main concept is to use powerful control intervention. Sliding mode approaches are one of the most effective methods to overcoming control problems, and they are gaining popularity. Emelyanov and several core searchers such as Utkins and Itkis proposed and developed VSC with SMC in the early 1950s in the Soviet Union. Significant interest in VSC and SMC has been developed in the control research community over the last decade[30] .

Sliding mode control (SMC) is a flexible control technique for variable structure systems (VSS) that provides robustness under parameter changes and external disturbances. It is a nonlinear control technique for keeping a plant's output(s) stable at a fixed point or on a specific trajectory. SMC is simpler to implement and has a greater degree of design versatility than other nonlinear controllers[31]. The design of a sliding surface in state space and the preparation of a control law to guide the system state trajectory starting from some arbitrary initial state to reach the sliding surface in finite time are two important steps in SM control. At the end, the system state trajectory should arrive at a point where the system equilibrium state occurs, which is in the origin point of the phase plane [32].There are two modes in a sliding mode controller (SMC). One is the reaching mode, in which the trajectory travels from some starting point towards the sliding surface. The system response is sensitive to parameter uncertainties and disturbances in reaching mode. The other is the sliding mode, in which the state trajectory follows the switching surface back to its origin, and the states never leave the switching line. [16]

Chattering: Unwanted fast oscillations of the system trajectories near the sliding surface are described as unwanted fast oscillations. The controlled system is vibrating at a dangerously high frequency. Any implementation of first order sliding mode control (1-SMC) must take this into account. Since every 1-SMC control signal is fast switching by default, it will cause chattering, which can excite unmolded high frequency dynamics, which is not accounted for in the design, and the device output will suffer, possibly leading to instability. When the control rule is applied in a sampled environment, as is most often the case, chattering occurs. Since sampled control systems operate as open-loop systems between sampling instants, no sampled control algorithm can satisfy a constraint with infinite precision when operating on a plant with unknown internal and/or external disturbances.

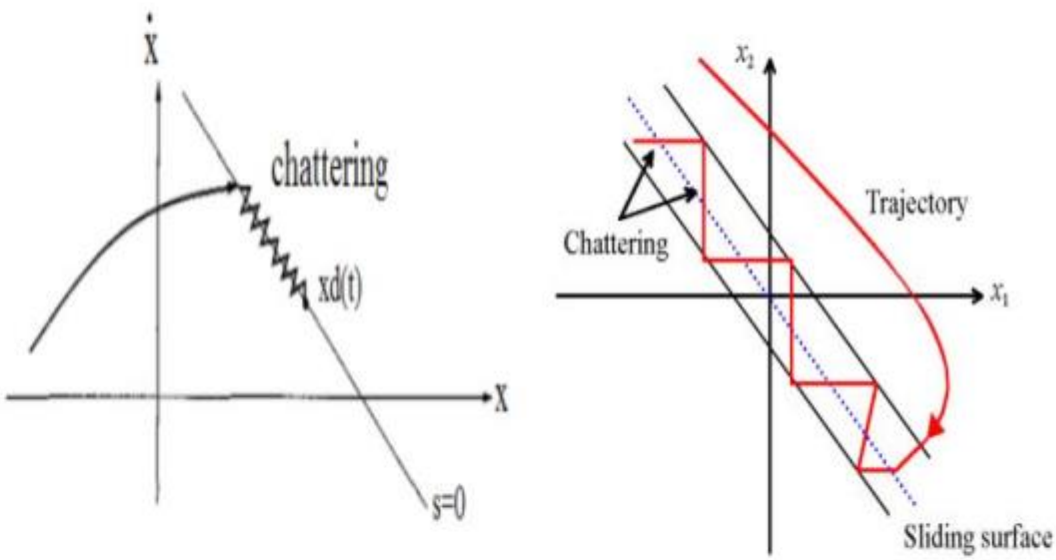

Figure 3.25: Chattering effect of SMC [33]

Instead of sign(s), the saturated function sat(s) s is now used to control the chattering effect.

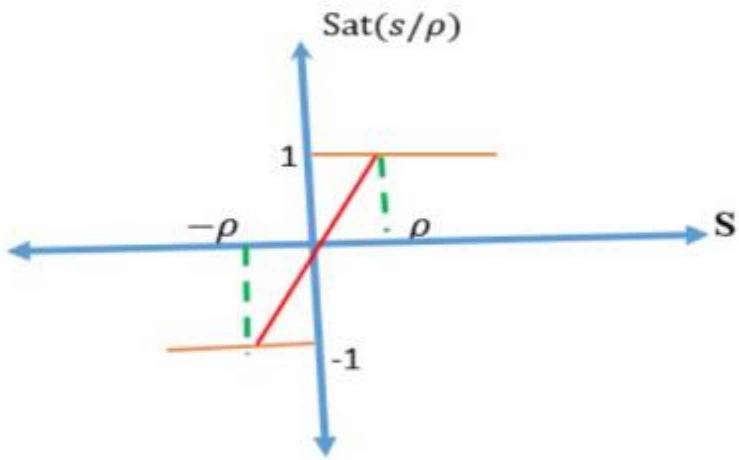

Figure 3.26: Saturation function [30]

$$\mathrm{Sat(s)} = \begin{cases} 1, & \text{for } s > \rho \\ \frac{s}{\rho}, & \mathrm{abs}(s) > \rho \\ -1, & s < \rho \end{cases} \tag{3. 96}$$

A. Sliding Mode Control of Switching Power Converters

The design and implementation of PWM-based SM voltage controllers are discussed in this part, with an emphasis on practical circuit design methodologies. It is not an easy undertaking, especially if the goal is to attain great accuracy while employing the smallest hardware available for the circuit design. A practical method to the design and selection of the controller's sliding coefficients is introduced in addition to the circuit design. This method, which is based on Ackermann's formula [34], allows for a systematic approach to control design. The controllers for these converters are analog in design, making them suited for industrial use. To validate the theoretical design, experiments are carried out.

B. PWM-based Sm Voltage Controller for Buck-Boost Converter

The implementation and design of the PWM-based SM voltage controller for buck-boost converters are covered in this part. The simulation work uses the same proportional-integral-derivative (PID) SM voltage controller as the previous section for consistency. The discussion is centered on the operation of the continuous conduction mode. The PWM-based SM voltage regulated buck-boost converter's schematic diagram is shown below.

Mathematical model

Existence conditions of buck-boost converters operating in CCM is shown below.

$$0 < \beta L\left(\frac{\alpha_1}{\alpha_2} - \frac{1}{r_L C}\right) i_C - LC\frac{\alpha_3}{\alpha_2}(V_{ref} - \beta \upsilon_O) < \beta \upsilon_O \tag{3. 97}$$

In addition, the derived control equations given as:

$$\upsilon_C = -\beta L\left(\frac{\alpha_1}{\alpha_2} - \frac{1}{r_L C}\right) i_C + LC\frac{\alpha_3}{\alpha_2}(V_{ref} - \beta \upsilon_O) + \beta \upsilon_O \tag{3. 98}$$

And

$$\hat{\upsilon}_{ramp} = \beta \upsilon_O \tag{3. 99}$$

Which are directly applicable for the implementation of the controller.

where R_L ,i_C maximum load resistance and is the maximum inductor current ripple during steady-state operation respectively.

The inequalities in (3.97) on the other hand, offer the criteria for existence and hence a range of sliding coefficients that will keep the converter in SM operation when its state trajectory is near the sliding surface.

Selection of Sliding Coefficients

Clearly, the inequalities above equation only provide broad information regarding the existence of SM, but no details about the parameter choices. It also provides no information on the relationship between the sliding coefficients and converter performance**.** We use Ackermann's method for building static controllers [34] for this purpose. This is essentially about choosing sliding coefficients based on the desired dynamic features. As a result, the system's stability criteria is automatically satisfied. This is a direct method of ensuring stability, with the same goal of ensuring that the eigenvalues of the Jacobian of the system in SM operation have negative real portions.

By substituting S = 0 into the equation relating the sliding coefficients to the dynamic response of the converter during SM operation in this section, the equation relating the sliding coefficients to the dynamic response of the converter during SM operation can be found.

$$\alpha_1 x_1 + \alpha_2 \frac{dx_1}{dt} + \alpha_3 \int x_1 dt = 0 \tag{3. 100}$$

We can get a standard second-order system form by rearranging the time differentiation of (3.100).

$$\frac{d^2x_1}{dt^2} + 2\xi\omega_n \frac{dx_1}{dt} + \omega_n{}^2 x_1 = 0 \tag{3. 101}$$

where $\omega_n = \sqrt{\frac{\alpha_3}{\alpha_2}}$ is the undamped natural frequency and $\xi = \frac{\alpha_1}{2\sqrt{\alpha_2\alpha_3}}$ is damping coefficient.

$$\frac{\alpha_3}{\alpha_2} = \frac{1}{4\xi^2}\left(\frac{\alpha_1}{\alpha_2}\right)^2 \tag{3. 102}$$

In a linear second-order system, there are mainly three types of responses: under-damped ($0 \leq \xi < 1$), critical damping ($\xi = 1$), and over-damped ($\xi > 1$).

(a) When SM operation is assumed for under-damped response converters, the output voltage error is given as

$$x_1(t) = A_1 \frac{e^{-\xi\omega_n t}}{\sqrt{1-\xi^2}} \cos\left(\omega_n \sqrt{1-\xi^2} t - \psi\right), \qquad \text{For } t \geq 0 \tag{3. 103}$$

The initial condition of the system and the phase angle $\psi = \arctan\frac{\xi}{1-\xi^2}$ determine A1. Because $\xi\omega_n$ determines the rate of decay in the response, the decay time constant is

$$\tau = \frac{1}{\xi\omega_n} = 2\frac{\alpha_2}{\alpha_1} \tag{3. 104}$$

Considering that the system settles to its steady state in 5τ seconds (1% criteria), the sliding coefficient ratio of α_1 and α_2 with regard to the settling time T_S is

$$\frac{\alpha_1}{\alpha_2} = \frac{10}{T_S} \tag{3. 105}$$

Tuning $\frac{\alpha_1}{\alpha_2}$ allows for the required settling time to be set. Furthermore, the peak oscillating overshoot for such systems is solely determined by the damping coefficient and is written as

$$\xi = \sqrt{\frac{\left[\ln\left(\frac{M_P}{100}\right)\right]^2}{\pi^2 + \left[\ln\left(\frac{M_P}{100}\right)\right]^2}} \tag{3. 106}$$

Where M_P is the percentage of the peak overshoot. As result, for a given desired overshoot, the damping coefficient ξ can be determined by using (3.104).

Substituting Equation (3.103) into Equation (3.100) and simplifying it gives,

$$\frac{\alpha_3}{\alpha_2} = \frac{25}{\xi^2 T_S^2} \tag{3. 107}$$

As a result, using the calculated and desired T_S, the required ratio for $\frac{\alpha_3}{\alpha_2}$ can be obtained.

(b) When the SM operation is as suggested for critically-damped response converters, the output voltage error is given as:

$$x_1(t) = (A_1 + A_2 t)e^{-\omega_n t}, \quad \text{for } t \geq 0 \tag{3. 108}$$

Where A1 and A2 are defined by the system's initial conditions

While ω_n determines the rate of decay in the response, the decay time constant is

$$\tau = \frac{1}{\omega_n} = \sqrt{\frac{\alpha_2}{\alpha_3}} \tag{3. 109}$$

Substituting Equation (3.100) into Equation (3.107) and simplifying it gives

$$\tau = 2\frac{\alpha_2}{\alpha_1} \tag{3. 110}$$

The appropriate sliding coefficient ratios are based on a 5 τ s (1 % criteria) settling time Ts.

$$\frac{\alpha_1}{\alpha_2} = \frac{10}{T_S} \text{ and } \frac{\alpha_3}{\alpha_2} = \frac{25}{{T_S}^2} \tag{3. 111}$$

(c) When SM operation is assumed for over-damped response converters, the output voltage error is given as

$$x_1(t) = A_1\left[\frac{-\xi+\sqrt{\xi^2-1}}{2\sqrt{\xi^2-1}}e^{\left(-\xi-\sqrt{\xi^2-1}\right)\omega_n t} - \frac{-\xi-\sqrt{\xi^2-1}}{2\sqrt{\xi^2-1}}e^{\left(-\xi+\sqrt{\xi^2-1}\right)\omega_n t}\right] \quad (3.\ 112)$$

$$\text{for } t \geq 0$$

Where A_1 is determined by the system's initial state. Two parameters $\left(-\xi-\sqrt{\xi^2-1}\right)\omega_n$ and $\left(-\xi+\sqrt{\xi^2-1}\right)\omega_n$ influence the rate of decay of the reaction in this case. For the purposes of calculating the settling time, it is sufficient to consider the slower of the two, i.e., $\left(-\xi-\sqrt{\xi^2-1}\right)\omega_n$. For this component, the decay time constant is

$$\tau = \frac{1}{\left(\xi-\sqrt{\xi^2-1}\right)\omega_n} = \frac{2}{1-\sqrt{1-\frac{1}{\xi^2}}}\frac{\alpha_2}{\alpha_1} \quad (3.\ 113)$$

The following equations can be developed from (3.111) and (3.100) assuming a 5 s (1 percent criteria) settling time Ts:

$$\frac{\alpha_2}{\alpha_1} = \frac{10}{\left(1-\sqrt{1-\frac{1}{\xi^2}}\right)T_S} \text{ and } \frac{\alpha_3}{\alpha_2} = \frac{25}{\left(\xi-\sqrt{1-\frac{1}{\xi^2}}\right)T_S{}^2} \quad (3.\ 114)$$

As a result, the ratios $\frac{\alpha_2}{\alpha_1}$ and $\frac{\alpha_3}{\alpha_2}$ can be calculated from for any required settling time and damping coefficient, for $\xi > 1$ using equation (3.112).

The 5 τ s (1 %) settling time assumed in the derivation is the time it takes for the controller to complete the SM operation phase, that is, the time it takes for the state trajectory S to track from any point on the sliding surface to steady-state equilibrium. This time duration excludes the reaching phase, which necessitates a short but finite time for S to move from an arbitrary point to the sliding surface (depending on the amount of the load or line disruption and the capacity of the energy storage elements). The total time required to complete both the SM operation phase and the reaching phase is theoretically equal to the converter's settling time Ts. In reality, however, because the time required to complete the SM operation phase is typically significantly longer than the time required to complete the reaching phase, it is sufficient to consider simply the SM operating phase's duration as the settling time. It should also be noted that the settling time description given above is only true for an ideal SM controller with an infinite switching frequency. Due to the non-ideality of the tracking motion, the settling time for a finite-switching-frequency SM controller, i.e., a PWM-based SM controller will be slightly longer than the ideal case.

As a result, the response's intended settling time as well as the type and quantity of damping required, as well as the existence of the relevant PWM-based controllers now determines the design of the sliding coefficients.

Implementation of controller

In many ways, the design of this controller includes selecting the desired frequency response's bandwidth, calculating the corresponding sliding coefficients, verifying compliance with the existence condition, and deriving the control equations by substituting the calculated parameters into (3.96) and (3.97).

Following that, we will go over the design process in detail.

Design procedure

Step 1: Using (3.103) and (3.105), or (3.109), or (3.112), the control parameters can be determined given a desired bandwidth. To check if the existence requirement is met.

Step 2: Given a reference voltage Vref, β the expression is calculated as follows:

$$\beta = \frac{V_{ref}}{V_{od}} \tag{3. 115}$$

Step 3: The gain required for signal amplification $(V_{ref} - \beta \upsilon_O)$ is $\frac{\alpha_3}{\alpha_2} LC$.

Step 4: Set the current sensing gain H to a value such that the measured capacitor current i_C(mea) equals the actual capacitor current i_C, and given that the controller is designed for maximum load current (i.e., minimum load resistance R_L(min)), the gain required for signal amplification is $\beta L \left(\frac{1}{R_L(\min) C} - \frac{\alpha_1}{\alpha_2} \right)$.

Step 5: The schematic diagram of the adaptive feedforward variable ramp generator used in our controller design is shown in this section.

Parameters of Controller

Simulations are used to validate the above-mentioned design strategy as well as the analog realization for the PWM-based SMVC buck-boost converter.

The converter's specifications are listed in Table 3.6.

Table 3.6: Specifications of buck-boost converter

Description	Parameter	Nominal Value
Input voltage	υ_i	12V
Capacitance	C	16.44μF
Capacitor ESR	c_r	50mΩ
Inductance	L	78.41 μH
Inductor resistance	l_r	0.01Ω
Switching frequency	f_S	100kHz
Maximum load resistance	R_L	14.4Ω
Desired output voltage	V_{Od}	24V

Signals at different test locations of a PWM-based SM controller are described theoretically

Test Location	Description
1	$K_{P1} i_C$
2	$-K_{P2}(V_{ref} - \beta \upsilon_O)$
3	$-\beta \upsilon_O$
4	V_C
5	$\hat{V}_{ramp}$
6	u_{PWM}
7	u_{CLK}
8	$u = u_{PWM} . u_{CLK}$

Simulation are conducted to validate the suggested specification of the PWM-based SMVC buck-boost converter. The PWM-based SMVC buck-boost converter simulation is implemented as shown in Table 3.6.

The SM controller is based on PWM and is developed to provide an under-damped response over a wide bandwidth ω_n = 10.1196 krad/s, i.e., τ = 0.8 ms and Ts = 2.2 ms, and damping coefficient ξ = 0.2. From above stated equation $\frac{\alpha_1}{\alpha_2} = 4545.54S^{-1}$ and $\frac{\alpha_3}{\alpha_2} = 5{,}165{,}289.256S^{-2}$ .It's important to note that we can verify that equation $\frac{\alpha_1}{\alpha_2} >> \frac{1}{R_L}$ for full-load conditions. The feedback divider ratio can be calculated as $\beta = \frac{V_{ref}}{V_{Od}} = \frac{1}{6}$ V/V if the controller's reference voltage is Vref = 4 V. Finally, the control parameters are established as follows:

$K_{P1} = \beta L\left(\frac{\alpha_1}{\alpha_2} - \frac{1}{r_L C}\right) = 0.1448\ Hs^{-1}$ and $K_{P2} = \frac{\alpha_3}{\alpha_2} LC = 0.358.$

CHAPTER FOUR

SIMULATION RESULTS AND ANALYSIS

The validity and stabilization of the proposed GA-fuzzy, GA-PID and SMC controllers for the DC-DC buck-boost converter are checked using simulation tools in this chapter. Matlab/Simulink software is used to run the simulation.

4.1 Open Loop Performance of Buck-Boost Converter

The buck-boost converter's open loop performance is evaluated and verified using the MATLAB/Simulink model shown in Figure 4.1. Table 4.1 shows the parameters that were used to conduct the simulation studies.

Table 4.1: Parameters used for the simulation purpose.

Description	Parameter	Nominal Value
Input voltage	v_i	12V
Capacitance	C	16.44μF
Capacitor ESR	c_r	50mΩ
Inductance	L	78.41 μH
Inductor resistance	l_r	0.01Ω
Switching frequency	f_S	100kHz
Maximum load resistance	R_L(max)	14.4Ω
Desired output voltage	V_{Od}	24V

Simulink Block Diagram of open loop Buck-Boost converter

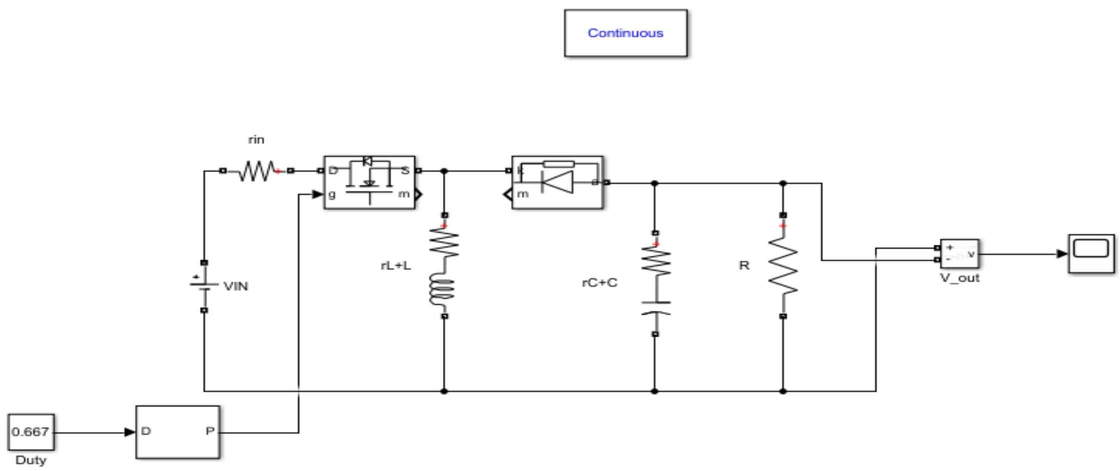

Figure 4. 1: MATLAB/Simulink model of open loop buck-boost converter

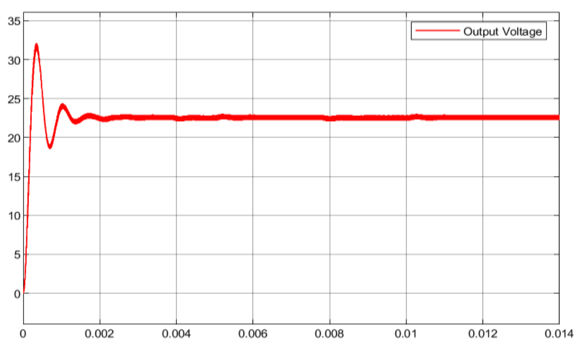

a) Open loop response on actual circuit

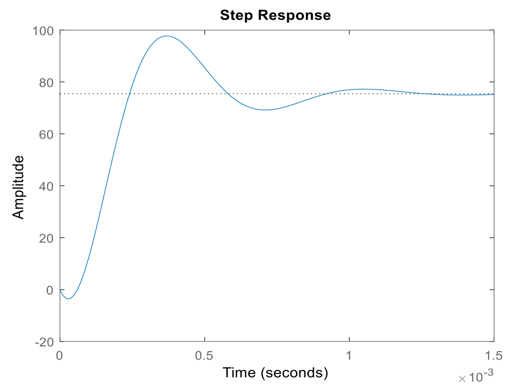

b) Open loop response using transfer function

Figure 4. 2: Output voltage of open loop buck-boost converter

The output voltage response obtained using MATLAB/Simulink is shown in Fig. 4.2 and it can be seen that it has a large unwanted overshoot, which is not necessary. As a result, effective controllers are needed to increase system performance and achieve fast, stable buck boost converter performance.

4.2 Performance of Buck-Boost Converter using PID Controller

The parameters of the buck-boost converter are the same as those listed in Table 4.1 to demonstrate the performance of a DC-DC buck-boost converter with a proportional integral derivative controller (PID) in MATLAB/Simulink. The variable to be regulated is output voltage, and the control input is error. Figure 4.3 shows a Simulink model of a buck-boost converter with a PID controller. PID Tuner is a fast and widely applicable tool in the MATLAB environment. Simulink PID controller blocks can be tuned using a single-loop PID tuning approach. The PID parameters Kp, Ki and Kd can be easily modified using this method to produce a robust design and the required reaction time.

Simulink block diagram of PID controller

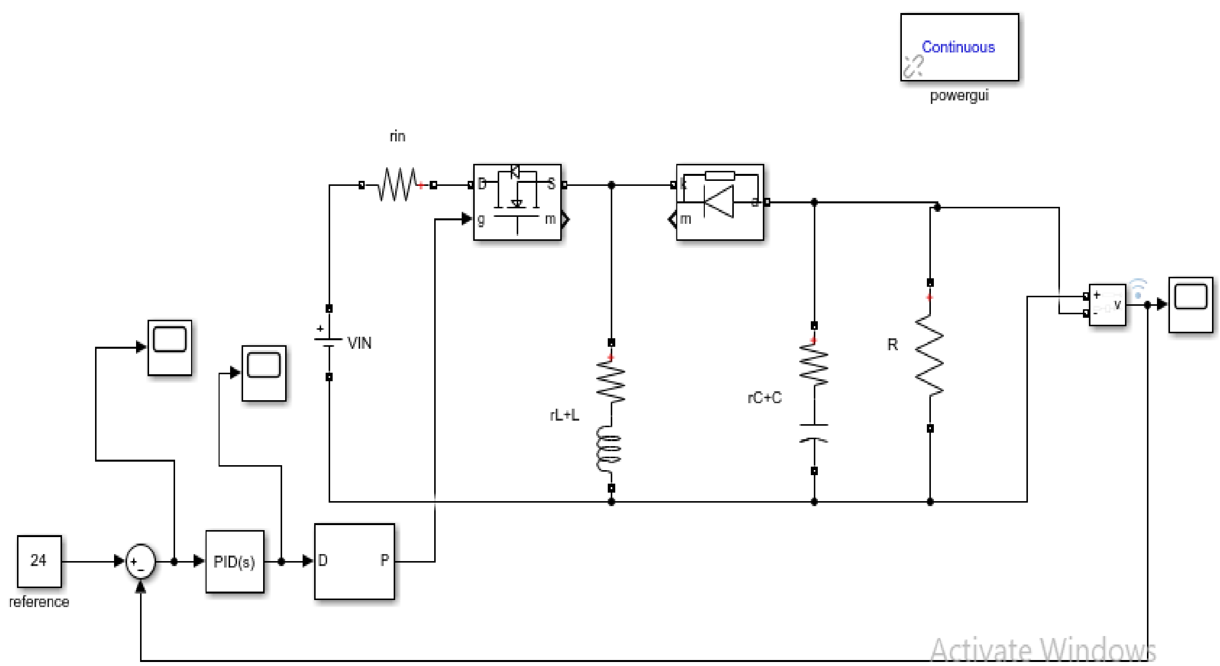

Figure 4. 3: Simulink block diagram of PID controller.

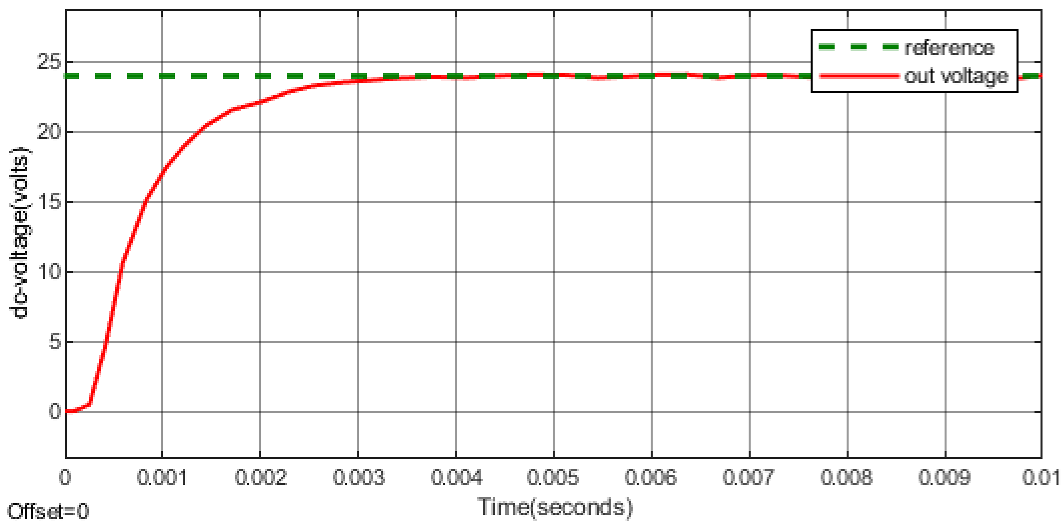

Figure 4. 4: voltage reference controller performance using PID controller

The output of the voltage controller of a DC-DC buck-boost converter employing PID controller is shown in figure (4.4). We can observe that the actual output voltage follows the desired output voltage from almost 0.00364 seconds to the end of the simulation time of 0.12 seconds.

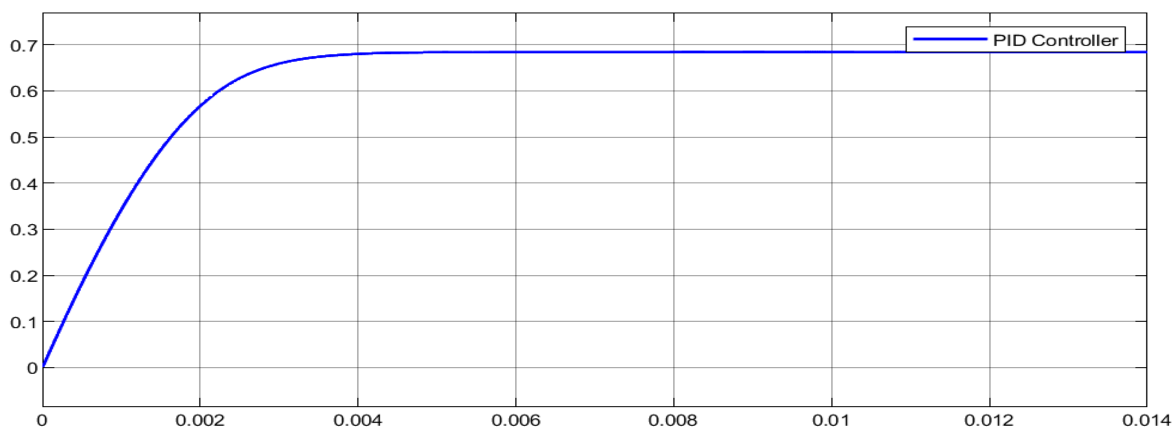

Figure 4. 5: PMW duty ratio control signal

Fig. (4.5) indicates that the regulated PWM duty ratio 0.667 is generated same as calculated in modeling and the controller acts effectively.

4.3 Performance of Buck-Boost Converter with PID Controller under Disturbance in Input Voltage and Load Resistance

In order to test the performance of DC-DC buck-boost converter with PID controller under input voltage change, the input voltage is increased from 12 to 15V and decreased to 9V respectively. In addition, to test the effect load resistance variation, the load resistance is increased from 14.4 to 17Ω and decreased to 10Ω respectively.

Simulink diagram of the converter with PID under the influence of disturbance

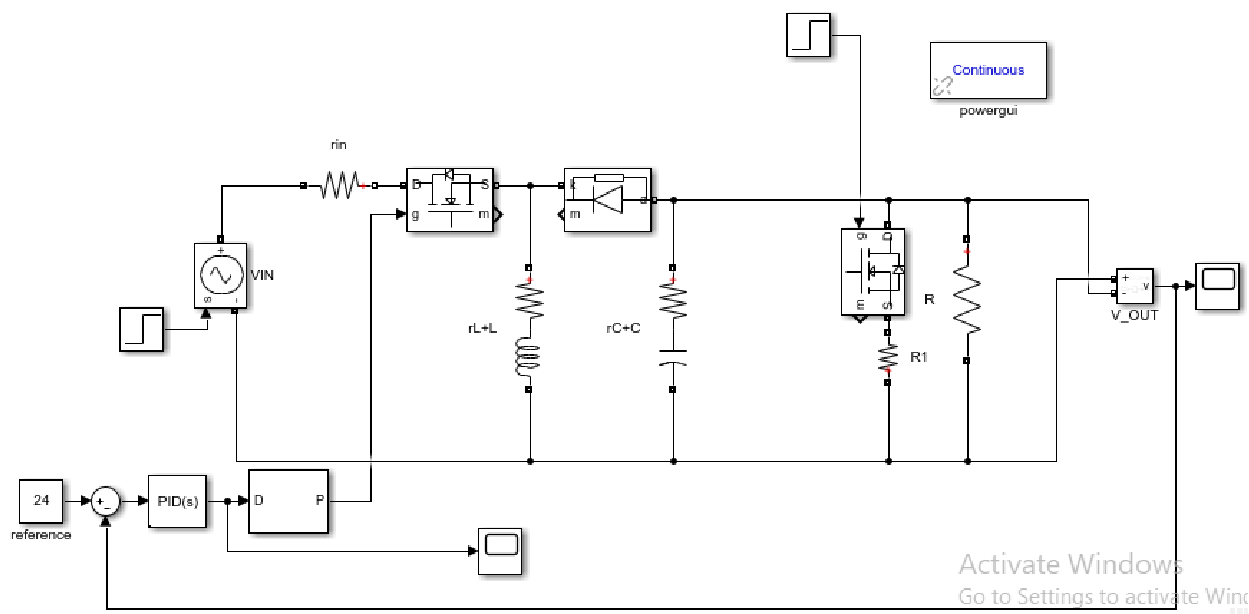

Figure 4. 6 Simulink diagram of the converter with PID under the influence of disturbance

When output of step block goes one the MOSFET close and cause the resistor R1 to be in parallel with resistor R from their setting time. By varying input voltage using controlled input and step block and varying load resistance output voltage response using this controller is disused .

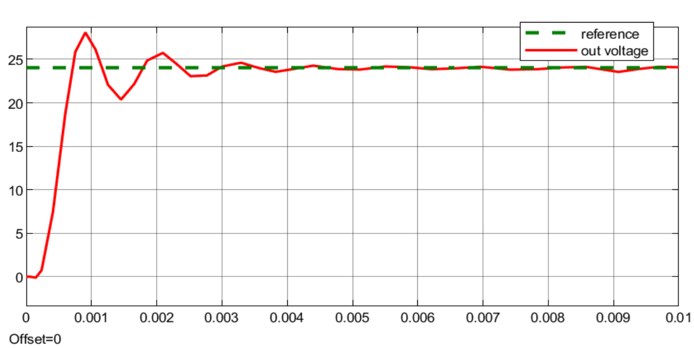

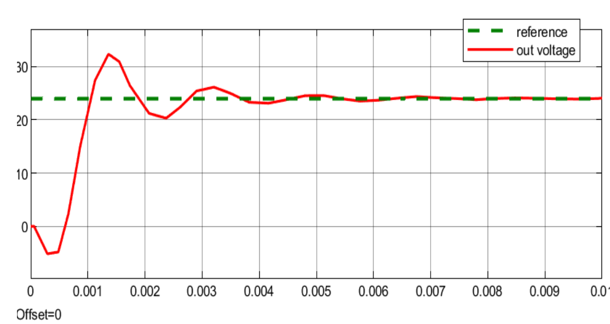

a) Input voltage change from 12 to 15V

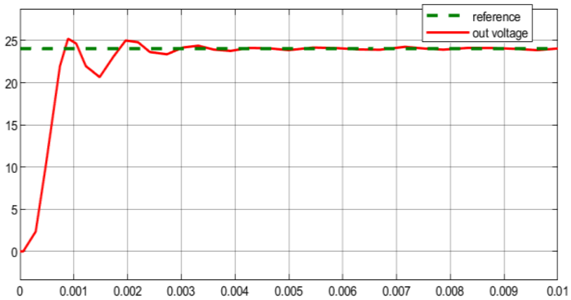

b) For input voltage change from 12 to 9V

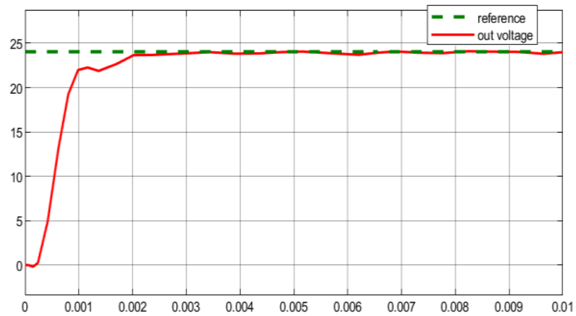

a) For load resistance change from 14.4 to 17 Ω

b) For load resistance change from 14.4 to 10Ω

Figure 4.7: Simulation results of buck-boost converter with PID under input voltage and load resistance variation

The simulation indicates that by minimizing the overshoot to a very small value while increasing the settling and rise time, the desired output voltage can be achieved using a PID controller for buck-boost converter (Figure 4.7).while buck-boost converter is nonlinear system, but in this case linear controller is designed based on small signal model of the converter after linearization. The controllers designed using this method were unable to respond to changes in operating point properly. As a result, nonlinear controllers are necessary to overcome the disadvantages of linear controllers.

4.4 Performance of Buck-Boost converter with GA-PID

The parameters of the converter are the same as those listed in Table 4.1 to demonstrate the performance of a DC-DC buck converter with GA-PID in MATLAB/Simulink.

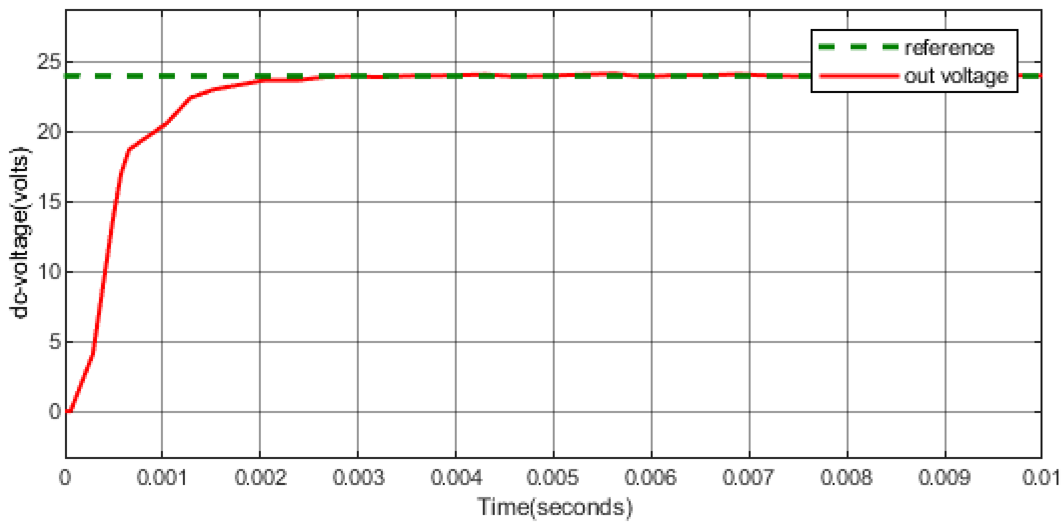

Figure 4.8: Output voltage of buck-boost converter with GA-PID.

From the result given in Figure 4.8 above, using GA-PID for buck-boost converter the overshoot is highly reduced. We can observe that the actual output voltage follows the desired output voltage from almost 0.001968 seconds to the end of the evaluation time of 0.01 seconds.

4.5 Performance of Buck-Boost Converter with GA-PID Controller under Disturbance in Input Voltage and Load Resistance

In order to test the performance of DC-DC buck-boost converter with GA controller under input voltage change, the input voltage is increased from 12 to 15V and decreased to 9V respectively. In addition, to test the effect load resistance variation, the load resistance is increased from 14.4 to 17Ω and decreased to 10Ω respectively. The simulation results are shown in Figure 4.9.

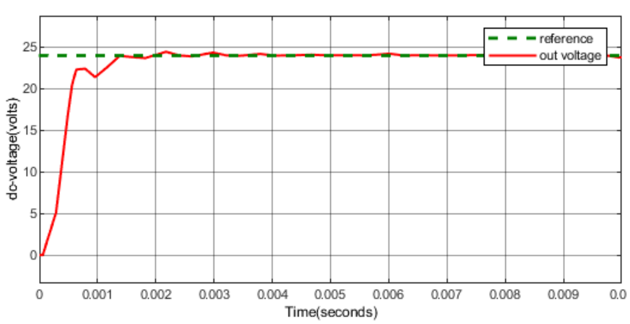

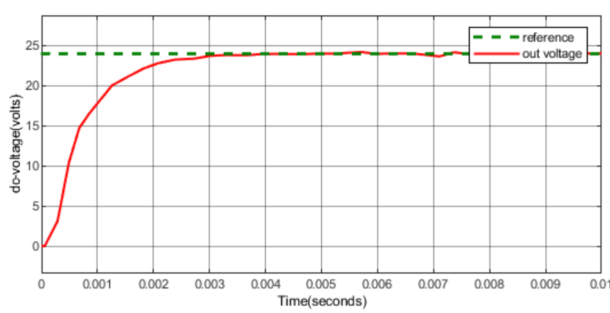

a) Input voltage change from 12 to 15V

b) For input voltage change from 12 to 9V

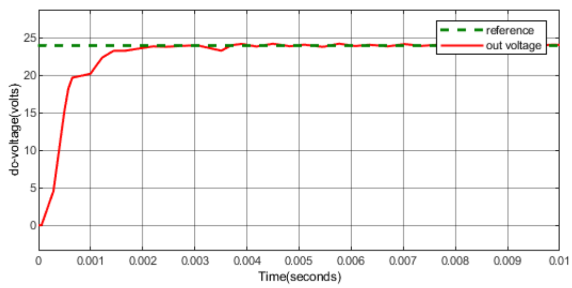

c) For load resistance change from 14.4 to 17 Ω

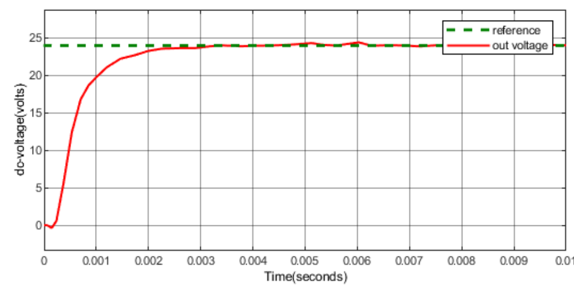

d) For load resistance change from 14.4 to 10Ω

Figure 4.9: Simulation results of buck-boost converter with GA-PID under input voltage and load resistance variation

The GA-PID designed for buck-boost converters, as shown in Fig. 4.9, tracks the desired output voltage under the effect of input change and load resistance variation. This demonstrates that the output voltage of a buck-boost converter is unaffected by load resistance variations when using a GA-PID, and that when an input change occurs on the system, the controller automatically takes corrective action to keep the system stable and reject disturbance effects. The designed controller is, as expected, robust.

4.6 Performance of Buck-Boost converter with GA-fuzzy

The parameters of the converter are the same as those listed in Table 4.1 to demonstrate the performance of a DC-DC buck converter with GA-fuzzy controller in MATLAB/Simulink. Figure 4.4 shows the Simulink model of a buck-boost converter with a GA-fuzzy controller.

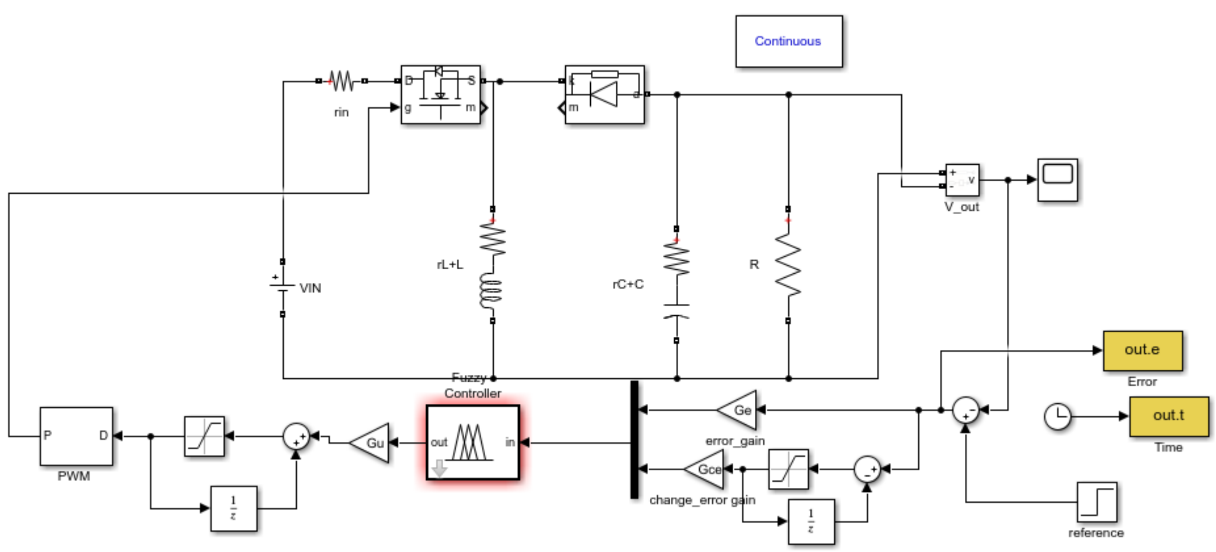

Figure 4. 10 Simulink diagram of the converter with GA-fuzzy controller

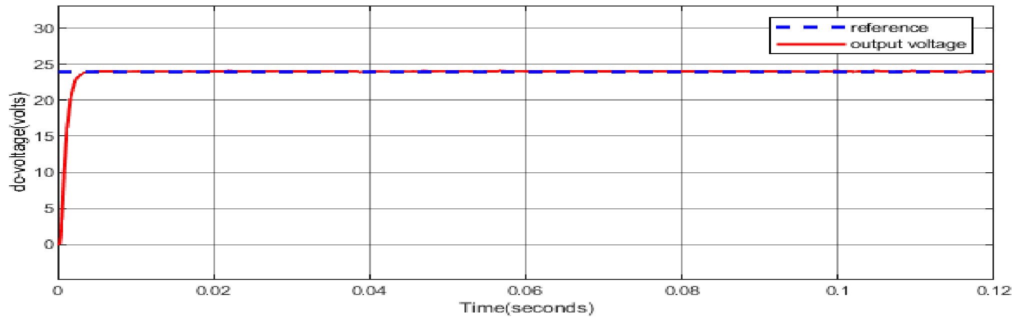

Figure 4.11: Output voltage of buck-boost converter with GA-fuzzy

4.7 Performance of Buck-Boost Converter with GA-fuzzy Controller under Disturbance in Input Voltage and Load Resistance

In order to test the performance of DC-DC buck-boost converter with GA-fuzzy controller under input voltage change, the input voltage is increased from 12 to 15V and decreased to 9V respectively. In addition, to test the effect load resistance variation, the load resistance is increased from 14.4 to 17Ω and decreased to 10Ω respectively. The simulation results are shown in Figure 4.12.

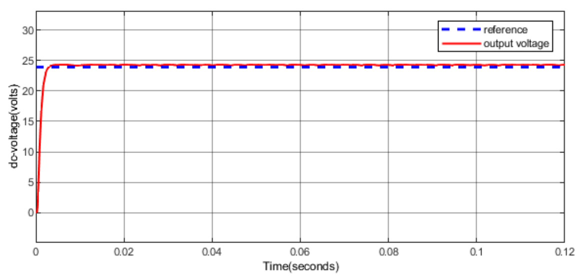

a) Input voltage change from 12 to 15V

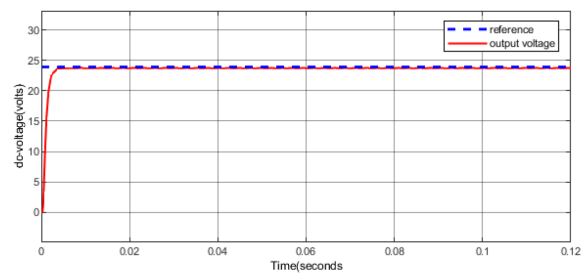

b) Input voltage change from 12 to 9V

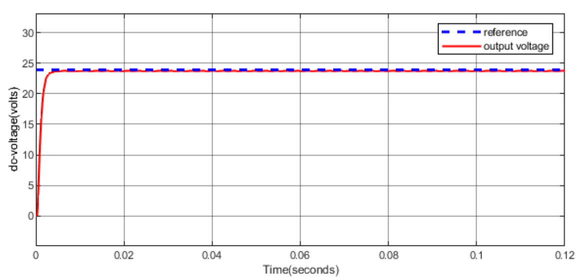

c) For load resistance change from 14.4 to 17 Ω

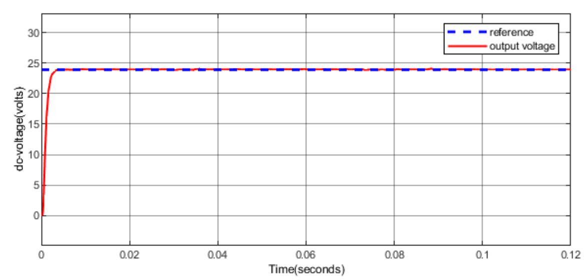

d) For load resistance change from 14.4 to 10 Ω

Figure 4.12: Simulation results of buck-boost converter with GA –fuzzy under input voltage and load resistance variation

According to the results shown in Figure 4.12, a DC-DC buck-boost converter using a GA-fuzzy can overcome input voltage and load resistance changes. The actual output voltage overlaps the desired output voltage with very small voltage oscillation. This indicates that the converter's output voltage is unaffected by input voltage or load resistance variations in order to produce the required output voltage. The output voltage of the buck-boost converter is unaffected by large input voltage variations by the GA-fuzzy controller, as shown in Figure 4.12. It shows that the actual output voltage of the converter overlaps the required output voltage for varying input voltages, implying that the desired output voltage is reached for significant input voltage variations

4.8 Performance of Buck-Boost Converter with sliding mode Controller

The parameters of the converter are the same as those listed in Table 4.1 to demonstrate the performance of a DC-DC buck-boost converter with sliding mode controller (SMC) in MATLAB/Simulink. Figure 4.13 shows a Simulink model of a buck-boost converter with an Sliding mode controller for a regulation problem with a resistive load.

Simulink block diagram of SMC for regulation problem

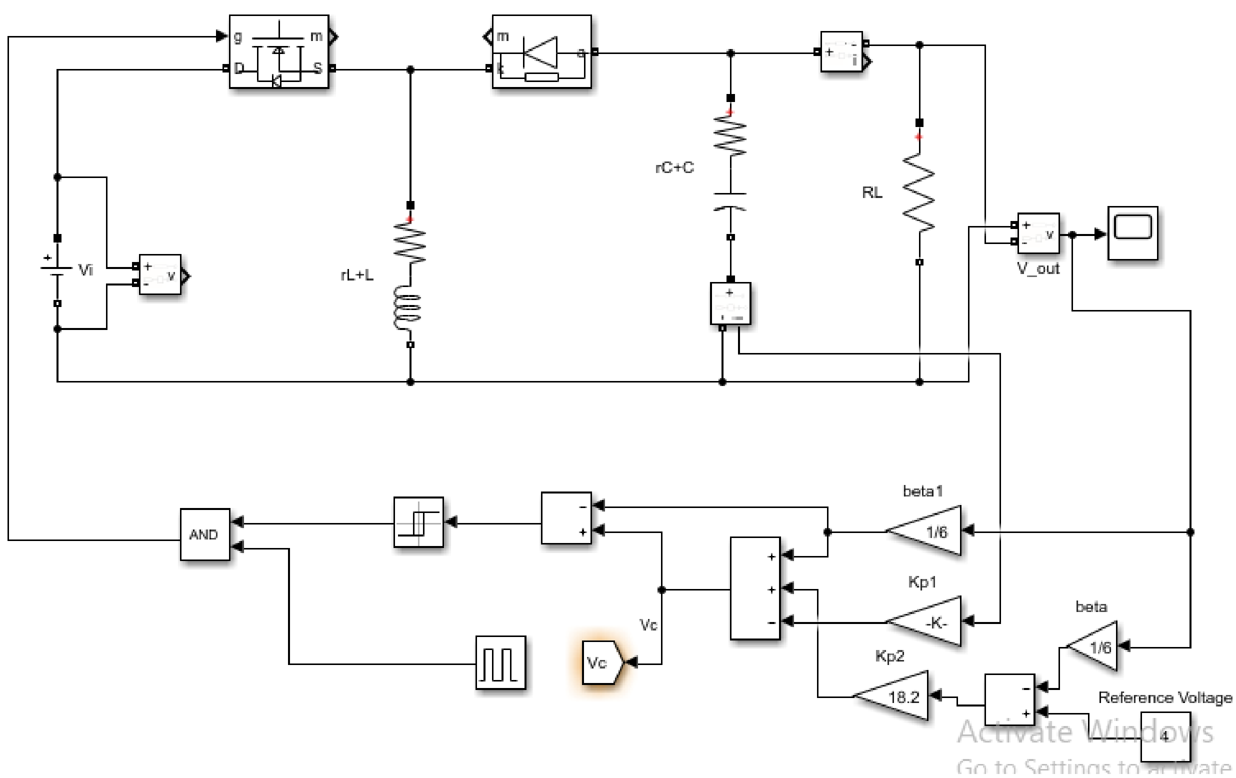

Figure 4.13: MATLAB/Simulink model of SM controller for voltage output regulation with resistive load.

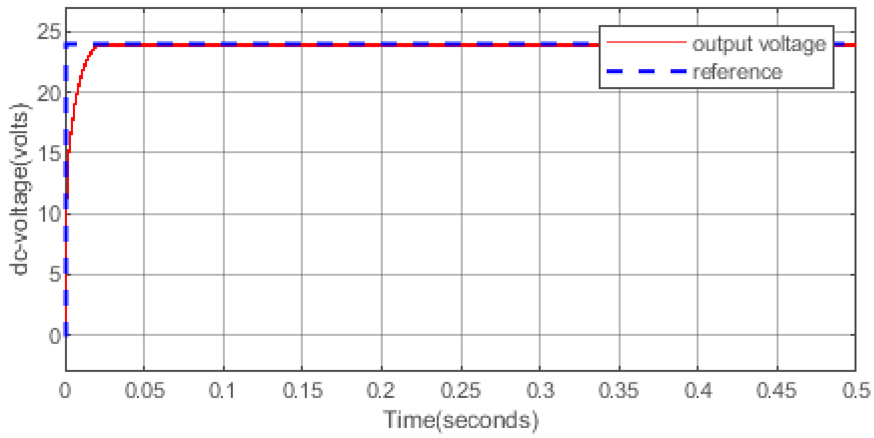

Figure 4.14: Output voltage regulation controller performance using SM controller

The result of the voltage controller of a DC-DC buck-boost converter using an SM controller is shown in figure (4.14). We can observe that the actual output voltage follows the desired output voltage from almost 0.01968seconds to the end of the simulation time of 0.5 seconds

4.9 Performance Comparison of GA-PID, GA-fuzzy and SM Controller for Buck-boost Converter

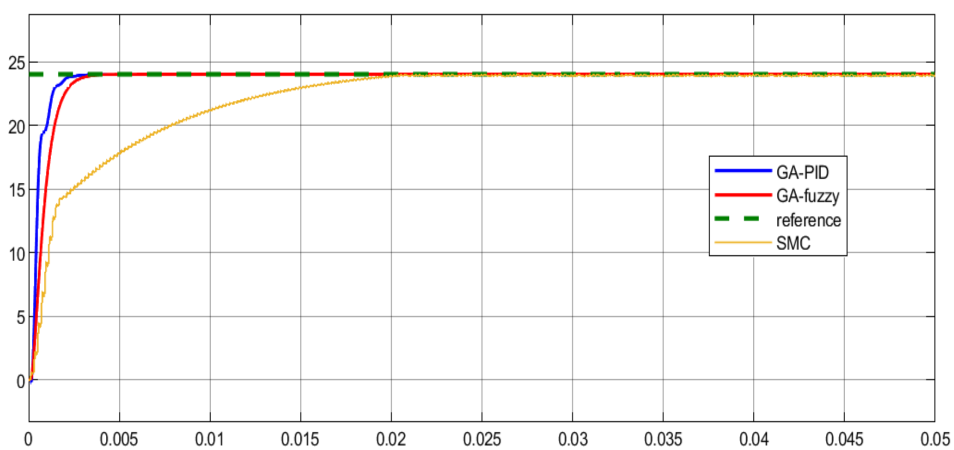

Figure 4.15: Output voltage of buck-boost converter with GA-PID, GA-fuzzy and SM controller

Figure 4.15 shows the responses of GA-PID control, GA-fuzzy control, and SM control when the buck-boost converter is required to provide the desired output voltage of 24V.It is clear that GA-fuzzy, control gives the desired output voltage more rapidly than GA-PID and SM control. GA-fuzzy control has a relatively small rising and settling time, but SM control have a long rise and settling time. As shown in Figure 4.15, the overshoot is reduced from 29.6 % to 0.132% when using GA-fuzzy controller, from 29.6% to 0.515% when using GA-PID controller, and from 29.6% to 0.312% when using sliding mode controller.GA-fuzzy controller is insensitive to input voltage and resistance variation. From simulation result, it is possible to conclude that the performance of GA-fuzzy controller is better than GA-PID and SM controller.

The transient performance and the output voltage deviation from desired value for input voltage variation is given in Table 4.2

Table 4.2: Result of transient performance and the output voltage deviation.

Controller	Rise time(in msec)	Settle time (in msec)	Overshoot %
GA-fuzzy	1.486	1.944	0.132
GA-PID	1.568	1.968	0.515
SMC	16.215	19.68	0.312

CHAPTER FIVE

CONCLUSIONS AND RECOMMENDATION

5.1. Conclusion

The key focus of this study is on three separate control methods for voltage regulation and tracking of DC-DC buck boost converters. The first control method is GA-fuzzy, while the second is based on the GA-PID and the third is using sliding mode control technique. Under load variation and input variation, the performance of DC-DC buck-boost converters was checked using MATLAB/Simulink for both controllers. It is clear that GA-fuzzy, control gives the desired output voltage more rapidly than GA-PID and SM control. GA-fuzzy control has a relatively small rising and settling time, but SM control have a long rise and settling time. The overshoot is reduced from 29.6 % to 0.132% when using GA-fuzzy controller, from 29.6% to 0.515% when using GA-PID controller, and from 29.6% to 0.312% when using sliding mode controller.GA-fuzzy controller is insensitive to input voltage and resistance variation..

A simulation is built using Matlab/Simulink to verify the controller's performance and quality. The controllers are designed to regulate the voltage of a buck-boost converter independently. The GA-fuzzy and SM is used to solve both the regulation and tracking problems, while the GA-PID is only used to solve the tracking problem. The controllers are effective, allowing them to regulate and monitor desired trajectories with ease. Finally, the controllers are measured on the voltage control variable using their performance such as settling time, rising time and overshoot. GA based fuzzy better performance with robust and stable. Since it is a nonlinear control, stable, and can compensate for the converter's nonlinearity, GA-fuzzy is improving rapidly in the application of DC-DC buck-boost converters.

5.2 Recommendation

While computer simulations have validated the theoretical of voltage regulation and monitoring of DC-DC buck-boost converters using GA based fuzzy, GA based PID and sliding mode control it may be useful to investigate its practical implementation. Furthermore, by incorporating a voltage controller for a particular application, a buck-boost converter plant can be made more accurate and appealing.

Another research topic is to introduce and test different nonlinear controllers, such as higher order sliding mode algorithms. A comparison of the output GA-fuzzy, GA-PID and sliding mode control designed with some other control mechanism should reveal new information.

Reference

[1] L. Gitleman, "NON LINEAR CONTROLLER FOR DC-DC BUCK CONVERTER," *Pap. Knowl. . Towar. a Media Hist. Doc.*, no. 1, pp. 1–19, 2014.

[2] "Gaussian Fuzzy Logic Control," no. July, 2012.

[3] M. Theses and R. Citation, "ScholarWorks at WMU Voltage Controller for Simulating Transition between Boost – Buck -Boost Converter," 2017.

[4] S. B. Padhyay, P. G. K. Panda, P. P. K. Saha, and P. S. Das, "Advance Control Techniques for DC/DC Buck Converter with Improved Performance," *Int. J. Adv. Res. Electr. Electron. Instrum. Eng.*, vol. 04, no. 01, pp. 201–208, 2015, doi: 10.15662/ijareeie.2015.0401029.

[5] K. F. Hussein, I. Abdel-Qader, and M. K. Hussain, "Hybrid fuzzy PID controller for buck-boost converter in solar energy-battery systems," *IEEE Int. Conf. Electro Inf. Technol.*, vol. 2015-June, pp. 70–75, 2015, doi: 10.1109/EIT.2015.7293323.

[6] M. D. Almawlawe and M. Kovandzic, "A Modified Method for Tuning PID Controller for Buck-Boost Converter," *Int. J. Adv. Eng. Res. Sci.*, vol. 3, no. 12, pp. 20–26, 2016, doi: 10.22161/ijaers/3.12.4.

[7] R. Marouani, K. Echaieb, and A. Mami, "Converter in PV Grid-Connected System," pp. 281–284, 2012.

[8] B. B. Naik and A. J. Mehta, "Sliding mode controller with modified sliding function for DC-DC Buck Converter," *ISA Trans.*, vol. 70, pp. 279–287, 2017, doi: 10.1016/j.isatra.2017.05.009.

[9] H. A. H. Ammar Falah Algamluoli, "Voltage Controller of DC-DC Buck Boost Converter with Proposed PID Controller," *Int. J. Adv. Res. Comput. Eng. Technol.*, vol. 9, no. 1, pp. 1–4, 2020.

[10] H. Guldemir, "Study of Sliding Mode Control of DC-DC Buck Converter," *Energy Power Eng.*, vol. 03, no. 04, pp. 401–406, 2011, doi: 10.4236/epe.2011.34051.

[11] S. Tyagi and G. Verma, "Simulation and Analysis of DC-DC Boost Converter Using

Sliding Mode Controller under Variable Conditions," vol. 13, no. 1, pp. 33–41, 2018, doi: 10.9790/1676-1301023341.

[12] A. Karthikayini, S. Ramprasath, and P. Rameshbabu, "Modeling and simulation of PWM based sliding mode voltage controller for Boost converter in continuous conduction mode," *IEEE Int. Conf. Circuit, Power Comput. Technol. ICCPCT 2015*, 2015, doi: 10.1109/ICCPCT.2015.7159358.

[13] M. A. F. Al-Qaisi, M. A. Shehab, A. Al-Gizi, and M. Al-Saadi, "High performance DC/DC buck converter using sliding mode controller," *Int. J. Power Electron. Drive Syst.*, vol. 10, no. 4, p. 1806, 2019, doi: 10.11591/ijpeds.v10.i4.pp1806-1814.

[14] B. A. Reddy and M. S. V. S. Kumar, "Automated Tuning and Controller Design for DC-DC Boost Converter," pp. 2–6, 2017.

[15] M. Sarvi, I. Soltani, and N. Rabbani, "A Sliding Mode Controller for DC/DC Converters Converters.," *Int. J. Eng. Sci. Res. Technol.*, vol. 1, no. 9, 2012.

[16] H. Guldemir, "Modeling and Sliding Mode Control of DC-DC Buck-Boost Converter," *6th Int. Adv. Technol. Symp.*, no. May, pp. 475–480, 2011.

[17] L. Guo, V. Nelson, R. Nelms, J. Hung, S. McFarland, and …, "Design and Implementation of Digital Controllers for Buck and Boost Converters …," 2006.

[18] "Fuzzy logic based sliding mode controlled DC-DC boost converter," *ICECE 2010 - 6th Int. Conf. Electr. Comput. Eng.*, no. December, pp. 70–73, 2010, doi: 10.1109/ICELCE.2010.5700555.

[19] M. S. Rahman, "Buck converter design issues," *Div. Electron. Devices Linkopings Univ.*, 2007, [Online]. Available: http://www.diva-portal.org/smash/record.jsf?pid=diva2:24104.

[20] N. Safari, "Design of a DC/DC buck converter for ultra-low power applications in 65nm CMOS Process," *Thesis*, no. March, 2012, [Online]. Available: http://liu.diva-portal.org/smash/record.jsf?pid=diva2:546843.

[21] E. Abbasi and M. Mahjoob, "Controlling of Quadrotor UAV Using a Fuzzy System for Tuning the PID Gains in Hovering Mode," *10th Int. Conf. Adv. Comput. Entertain.*

Technol., no. September, pp. 1–6, 2013, [Online]. Available: http://conf-scoop.org/ACE-2013/13_Reza2_ACE.pdf.

[22] F. L. Lewis, *Dynamics and Control of Fixed-wing UAV Dynamics and Control of Fixed-wing UAV*. .

[23] R. Ildarabadi and A. Ahmadi, “A Review to AC Modeling and Transfer Function of DC-DC Converters,” *TELKOMNIKA Indones. J. Electr. Eng.*, vol. 13, no. 2, 2014, doi: 10.11591/telkomnika.v13i2.7033.

[24] G. V. Mohammed Dahleh, Munther A.Dahleh, *_Letures on Dynamic Systems and Control*. .

[25] A. V. Daware and A. Sabnis, “Performance Measurement of Linear and Non Linear Controllers for Buck-Boost Converter in Solar Energy System,” *7th IEEE Int. Conf. Comput. Power, Energy, Inf. Commun. ICCPEIC 2018*, no. 3, pp. 225–229, 2018, doi: 10.1109/ICCPEIC.2018.8525210.

[26] D. Sivamani, R. Harikrishnan, and R. Essakiraj, “Genetic algorithm based PI controller for DC-DC converter applied to Renewable energy applications,” *Int. J. Pure Appl. Math.*, vol. 118, no. 16, pp. 1053–1071, 2018.

[27] “2012 IEEE International Conference on Power Electronics, Drives and Energy System2012 IEEE International Conference on Power Electronics, Drives and Energy Systems December16-19, 2012, Bengaluru, Indias December16-19, 2012, Bengaluru, India,” no. 3, 2012.

[28] A. G. Perry, G. Feng, Y. F. Liu, and P. C. Sen, “A new design method for PI-like fuzzy logic controllers for DC-to-DC converters,” *PESC Rec. - IEEE Annu. Power Electron. Spec. Conf.*, vol. 5, pp. 3751–3757, 2004, doi: 10.1109/PESC.2004.1355138.

[29] M. A. Kaabar, “Design of GA-Fuzzy Controller for Buck DC-DC Converters,” 2014.

[30] J. Liu, *Sliding mode control using MATLAB*. 2017.

[31] B. Mariam David, “A Review of Sliding Mode Control Of DC-DC Converters,” *Int. Res. J. Eng. Technol.*, pp. 1382–1386, 2015.

[32] S. Verma, S. K. Singh, and A. G. Rao, “Overview of control Techniques for DC-DC converters,” *Res. J. Eng. Sci.*, vol. 2, no. 8, pp. 18–21, 2013.

[33] C. Cömert and C. Kasnakoglu, “Comparing and Developing PID and sliding mode Controllers for Quadrotor,” *Int. J. Mech. Eng. Robot. Res.*, vol. 6, no. 3, pp. 194–199, 2017, doi: 10.18178/ijmerr.6.3.194-199.

[34] J. Ackermann and V. Utkin, “Sliding mode control design based on Ackermann’s formula,” *IEEE Trans. Automat. Contr.*, vol. 43, no. 2, pp. 234–237, 1998, doi: 10.1109/9.661072.

Appendix

A: Parameter Specification of Buck-Boost Converter

The parameters for buck-boost converters are based on equations and are optimized for low power and high switching frequency applications. As a result, the values for the converter parameters used in MATLAB/Simulink are as follows:

- The switching frequency is 100 kHz.
- The input voltage 12V.
- The desired output voltage is 24V.
- The load resistance is calculated as 14.4Ω.
- Assume the capacitor ripple voltage is 0.4%.

It is now possible to determine the minimum inductor that defines the boundary between continuous and discontinuous conduction modes using these parameters. We may also calculate the minimum capacitor to keep the ripple voltage below a specified level and reduce overshoot. We can calculate the duty cycle using the above value.

$$D = \frac{V_O}{V_{in}}(1 - D) = 0.67$$

Then the minimum inductor given as:

$$L_{min} = \frac{(1-D)^2}{2f}R = 7.841\ \mu\text{H}$$

Because the buck-boost converter is only designed for continuous conduction, the inductor value may be higher than the minimal value. Then, to assure continuous conduction mode of operation, set the inductor's value to ten times its minimum value, so L=78.41 μH. The required minimum capacitance is computed as follows:

$$C_{min} = \frac{(1-D)V_O}{\Delta V_O L f^2} = 13.15\mu F$$

The value capacitor should be bigger than the minimum value to reduce voltage overshoot and keep the peak to peak voltage ripple value below a specific level. As a result, let the value capacitor be increased by 25% of the capacitor's minimum value, resulting in C=16.44μ F

B: GA code for fuzzy

```
function Tune_PIDModel1_SPB

clear all

options= optimoptions('ga','PlotFcn',@gaplotbestf);

options.PopulationSize= 40;

options.MaxGenerations= 30;  % Increase value if needed

nvar= 3; % Number of parameters

LB= [0 0 0]; % Lower bound of tuning parameters

UB= [5 5 10]; % Upper bound of tuning parameters

[x,fval]= ga(@EvalObj,nvar,[],[],[],[],LB,UB,[],options)

% Updates Kp, Ki and Kd in simulink model workspace for verification

simulink_model= 'PIDModel1_SPB';

load_system(simulink_model);

gains= get_param(simulink_model,'modelworkspace');

gains.assignin('Ge', x(1));

gains.assignin('Gce', x(2));

gains.assignin('Gu', x(3));

% EvalObj measures a performance index from the simulink model for tuning

% obj= EvalObj(x) returns the objective function value obj calculated using

% the gain vector, x= [Kp Ki Kd].

function obj= EvalObj(x)

% Updates the values of Kp, Ki and Kd in Simulink model workspace

simulink_model= 'PIDModel1_SPB';
```

```
load_system(simulink_model);
gains= get_param(simulink_model,'modelworkspace');
gains.assignin('Ge', x(1));
gains.assignin('Gce', x(2));
gains.assignin('Gu', x(3));
% Simulates the simulink model to get the outputs
simOut= sim(simulink_model,'SaveOutput','on');
% Retrieves time t and error e
t= simOut.find('t');
e= simOut.find('e');
% Calculate a performance index using the trapezoidal integration rule
n= length(e);
ee= abs(e);
obj= 0;
for i= 2:n
   stepsize= t(i)-t(i-1);
   obj= obj+0.5*(ee(i-1)+ee(i))*stepsize; % IAE
%    obj= obj+0.5*t(i)*(ee(i-1)+ee(i))*stepsize; % ITAE
%    obj= obj+0.5*(ee(i-1)^2+ee(i)^2)*stepsize; % ISE
end
```